RIGA TECHNICAL UNIVERSITY

Marika Ščeglova

GALLIUM CONTAINING CALCIUM PHOSPHATES

Summary of the Doctoral Thesis

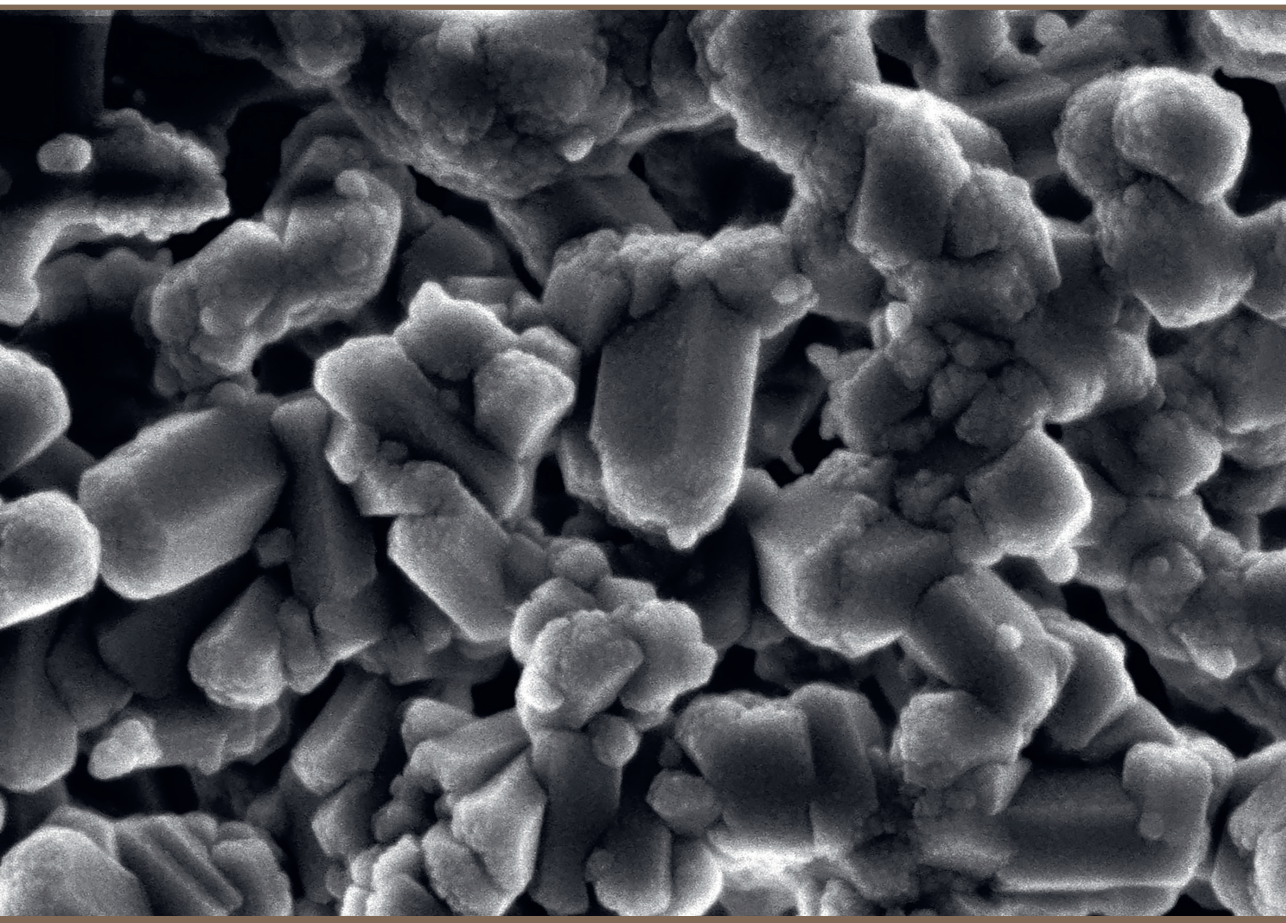

RTU Press
Riga 2026

RIGA TECHNICAL UNIVERSITY
Faculty of Natural Sciences and Technology
Institute of Biomaterials and Bioengineering

Marika Ščeglova
Doctoral Student of the Study Programme "Chemistry, Materials Science and Engineering"

GALLIUM CONTAINING CALCIUM PHOSPHATES

Summary of the Doctoral Thesis

Scientific supervisors
Professor Dr. sc. ing
JĀNIS LOČS

Senior Researcher Dr. sc. ing.
LĪGA STĪPNIECE

RTU Press
Riga 2026

Ščeglova, M. Gallium Containing Calcium Phosphates. Summary of the Doctoral Thesis. – Riga: RTU Press, 2026. –38 p.

Published in accordance with the decision of the Promotion Council "RTU P-02", January 26, 2026, Minutes No 04030- 9.2/3.

The Doctoral Thesis research was supported by the European Union`s Horizon 2020 research and innovation programme under grant agreements No. 857287 (BBCE), No. 952347 (RISEus2), and EuroNanoMedIII project "NANO delivery system for one-shot regenerative therapy of peri-implantis" (ImplantNano)**,** No. ES RTD/2020/19**.**

Cover image by Krišjānis Šmits.

https:/doi.org/10.7250/9789934372759
ISBN 978-9934-37-275-9 (pdf)

ACKNOWLEDGEMENTS

I would like to express my sincere gratitude to my family. My husband Artemijs for believing in me more than I believed sometimes in myself, for the support, encouragement and discussions outside of working hours. I am beyond grateful to share this journey and these accomplishments with him. Thanks to my biggest gift and motivator – my son Adrian, to my mother Galina, my mother-in-law Jelena, my nieces Arina, Sofia and Marija for believing in my strength and being there for me!

My heartfelt thanks to my friend Kristīne for support, encouragement, and the effort to understand what I do, for "the push" in those times when I felt like quitting!

Huge thanks to Renāts, an excellent student, for his dedication and responsiveness, and for being there for me in the laboratory.

To my esteemed colleagues at IBB for inspiring stories and fruitful scientific discussions, and their contribution to the creation of this Thesis. Additionally, I would like to sincerely thank Dr Nicola Dobelin for his valuable collaboration and for sharing his expertise with me.

Deepest gratitude to my supervisors, Senior Researcher Dr. sc. ing. Līga Stīpniece for her support, scientific ideas and Professor Dr. sc. ing Jānis Ločs, for the mentorship and knowledge provided!

In conclusion, I want to acknowledge myself for not giving up, moving through fears, challenges and self-doubt. This Thesis is not only about obtaining a degree but also about resilience and unwavering commitment to success.

"There is nothing to fear, because you cannot fail – only learn, grow, and become better than you've ever been before."

Hal Elrod

DOCTORAL THESIS PROPOSED TO RIGA TECHNICAL UNIVERSITY FOR PROMOTION TO THE SCIENTIFIC DEGREE OF DOCTOR OF SCIENCE

To be granted the scientific degree of Doctor of Science (PhD), the present Doctoral Thesis has been submitted for defence at the open meeting of RTU Promotion Council on April 24, 2026, at the Faculty of Natural Sciences and Technology of Riga Technical University, Paula Valdena street 3/7, room 272.

OFFICIAL REVIEWERS

Docent Dr. sc. ing. Gerda Gaidukova
Riga Technical University

Docent Dr. sc. ing. Agnese Brangule
Riga Stradiņš University, Latvia

Professor PhD Anna Tampieri
Institute of Science, Technology and Sustainability for Ceramics, Italy

DECLARATION OF ACADEMIC INTEGRITY

I hereby declare that the Doctoral Thesis submitted for review to Riga Technical University for promotion to the scientific degree of Doctor of Science is my own. I confirm that this Doctoral Thesis has not been submitted to any other university for promotion to a scientific degree.

Marika Ščeglova …… (signature)
Date: ……

The Doctoral Thesis has been prepared as a collection of thematically related scientific publications, completed by summaries in Latvian and English. The Doctoral Thesis unites four scientific publications. The scientific publications have been written in English, totaling 92 pages, including supplementary data.

TABLE OF CONTENTS

LIST OF ABBREVIATIONS

ACP – amorphous calcium phosphate
BET – Brunauer–Emmett–Teller method
CaP – calcium phosphate
CDHAp – calcium-deficient hydroxyapatite
DI – deionized
DMEM – Dulbecco's modified Eagle's medium
DSC – differential scanning calorimetry
FTIR – Fourier transform infrared spectroscopy
GaACP – gallium containing amorphous calcium phosphate
GaCaP – gallium containing calcium phosphate
GaHAp – gallium containing hydroxyapatite
HAp – hydroxyapatite
hTERT BJ1 – telomerase-immortalised human foreskin fibroblasts
ICDD – International Centre for Diffraction Data
OD_x – optical density (x – the wavelength at which the OD was measured, nm)
PBS – phosphate buffer saline
SCI – Science Citation Index
SEM/STEM – scanning electron microscopy/scanning transmission electron microscopy
SSA – specific surface area
TCP (α, β) – tricalcium phosphate (α, β)
TGA – thermogravimetric analysis
TSB – tryptic soy broth
XRD – X-ray diffraction

GENERAL OVERVIEW OF THE THESIS

Introduction

Bone is a composite material with a heterogeneous, anisotropic, and hierarchical structure. Its extracellular matrix consists of organic components (~ 30 %, mainly collagen fibril arrays) and an inorganic component (~ 70 %, composed primarily of nonstoichiometric hydroxyapatite (HAp) or biological apatite nanocrystals arranged within the collagen fibrils) [1]–[4]. The pathways of biological apatite formation are still unclear. One of the leading hypotheses proposes that the process begins with the amorphous calcium phosphate (ACP) *Posner* clusters, which transform into low-crystalline apatite [5]–[7]. Bone can regenerate itself. Namely, when bone gets damaged, it can naturally remodel through the coordinated actions of osteoclasts, osteoblasts, and osteocytes. However, defects that are critical in size (> 2 cm [8]) require additional treatment. Nevertheless, injuries, illnesses, or long-standing conditions such as osteoporosis and diabetes can hinder the healing process.

Regenerative medicine and bone tissue engineering offer a promising approach to enhance natural healing or replace damaged tissues using biomaterial implants and devices. One of the strategies involves using calcium phosphate (CaP) biomaterials, which are osteoconductive, biocompatible, and have high osseointegration ability [9]. Furthermore, CaP bioceramics can provide controlled biodegradation through the dissolution-precipitation process, allowing integration and replacement of the implant material with the new bone tissue [10], [11]. They can be produced in various forms, including powders, pellets, and scaffolds [12], [13]. Moreover, their versatility in composition, porosity, and mechanical properties allows customisation to meet specific application requirements [14], [15].

HAp is the most widely used CaP phase in the biomaterial field due to its chemical and structural similarity to the native bone tissues [16], [17]. Its chemical formula is $Ca_{10}(PO_4)_6(OH)_2$, and Ca/P molar ratio is 1.67 [18]. HAp possesses high thermodynamic stability and low solubility (pKsp 117.3 (at 37 °C) [19]). On the other hand, ACP is a metastable phase characterised by a short-range atomic order structure with chemical formula $Ca_xH_y(PO_4)_z{\cdot}nH_2O$ (Ca/P molar ratio 1.5) [20], [21]. Besides, it serves as a precursor phase in the precipitation process of other CaPs [21]. ACP offers advantages over HAp, such as higher solubility and faster resorption rate attributed to its hydrated layer and lack of crystallinity [22], [23].

Nowadays, tissue regeneration has become more predictable, addressing and satisfying the diverse needs of patients due to the advancement of the biomaterial field. However, any biomaterial possesses a risk of infection, as the properties that make them suitable for use in living organisms also create favourable conditions for bacteria. In orthopaedic surgeries, the primary complication is biomaterial-associated infections, especially in hip and knee replacements [24]. For instance, the rate of periprosthetic joint infections ranges from 0.7 % to 4 %, but after revision surgery, this rate can rise up to 20 % [25]–[31]. The predominant pathogens involved are gram-positive bacteria, with *Staphylococcus aureu*s (*S. aureus*) causing 33–43 % of infections and *Staphylococcus epidermidis* (*S. epidermidis*) being responsible for

17–21 % of cases [30], [32], [33]. Gram-negative bacteria, such as *Pseudomonas aeruginosa (P. aeruginosa)*, are less frequent and account for approximately 6 % of cases [34]. Systematic antibiotic administration is the traditional approach to treating biomaterial-associated infections. Still, it often results in systemic toxicity, low drug accumulation in the target site, and contributes to antibiotic resistance, especially in the case of *P. aeruginosa*. Consequently, antibiotics are ineffective against biofilms, which are a major cause of implant failure [33].

Before the discovery of antibiotics, different metals and their ions were used as antibacterial agents [35], [36]. It has paved the way for modern strategies, including modifying biomaterials with metal ions to enable long-term local ion release, providing antibacterial action at the defect site [37]. Commonly used metal ions for these modifications include silver (Ag^{+}), zinc (Zn^{2+}), strontium (Sr^{2+}), sodium (Na^{+}), and copper (Cu^{2+}), among others, which have demonstrated antibacterial activity against various pathogens [38]. Additionally, biologically relevant metal ions such as calcium (Ca^{2+}), iron (Fe^{2+}), magnesium (Mg^{2+}), and manganese (Mn^{2+}) play a crucial role in bacterial protein metabolism and overall physiological functions [39], [40].

Literature Review (Paper 1)

Gallium (Ga) and its compounds have been studied since the 1970s and have recently gained interest as therapeutic agents due to their antibacterial [41], [42], antitumor [43], and anti-inflammatory [44] properties. Unlike conventional antibiotics, Ga^{3+} ions can target tumours and infectious sites without inducing drug resistance [45]. Ga^{3+} ion has demonstrated antibacterial efficacy against both gram-positive and gram-negative bacteria, primarily due to its ability to mimic Fe^{3+} in bacterial metabolism (Fig. 1) [46], [47]. This "*Trojan horse*" strategy involves Ga^{3+} being "mistakenly" incorporated into bacterial iron-dependent processes, such as transferrin, heme-containing proteins, and siderophores [48]–[50]. As a result, bacterial metabolism is disrupted, leading to impaired DNA synthesis, respiration, and oxidative stress responses.

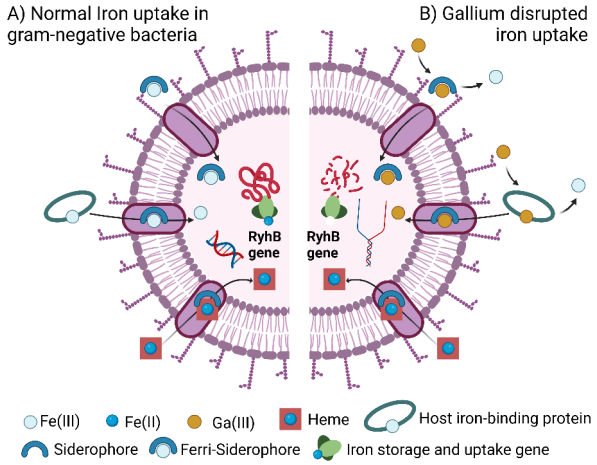

Fig. 1. A – Normal iron uptake metabolism in gram-negative bacteria; B – gallium disrupted iron uptake metabolism in gram-negative bacteria (adapted from [51], created with *Biorender.com*) [52].

A suitable carrier is required to deliver Ga^{3+} ions directly into the surgical site. Accordingly, Ga-containing CaPs (GaCaPs) can serve as controlled-release carriers for localised therapeutic action. Of the wide range of CaPs, only a few representatives have been modified with Ga, i.e., ACP, HAp, and β-tricalcium phosphate (β-TCP).

Up to now, only one study had documented Ga-containing ACP (GaACP) produced through the sol-gel method, showing antibacterial activity against *P. aeruginosa* as the (Ca + Ga)/P molar ratio increased [53]. However, this study did not cover an investigation into the stability of GaACP and antibacterial activity against other bacterial species. Regarding Ga-containing HAp (GaHAp), several studies have been reported in scientific literature. Usually, the low-crystallinity HAp with Ga content ranging from 0.33 wt% to 13 wt% has been synthesised using various synthesis methods. It has been reported that GaHAp exhibits antibacterial properties against *P. aeruginosa*, *Pseudomonas fluorescens* (*P. fluorescens*) [54]–[56]. Nonetheless, the existing literature does not address high-temperature GaHAp bioceramics, and the comprehension of Ga substitution remains limited [53].

From the literature review, it was concluded that the synthesis method and processing of the precipitates significantly influence the incorporation of Ga into the CaPs' crystalline structure, impacting the Ga^{3+} ion release profile and biological performance of CaPs. Thus, the Thesis concentrated on conducting systematic research regarding the influence of Ga on the properties of CaPs, highlighting the scarcity of studies concerning the stability of GaACP and the GaHAp bioceramics produced at various sintering temperatures. In the Thesis, the stability and antibacterial properties of GaACP were assessed, the *in vitro* antibacterial activity and cytotoxicity of GaHAp were examined, and high-temperature GaHAp bioceramics were prepared and characterised.

Aim and Objectives

The Thesis aimed to investigate the influence of gallium ions on the physicochemical properties of amorphous calcium phosphate and hydroxyapatite and to explore *in vitro* biological properties of the obtained materials. To achieve this aim, the following objectives were set.

1. To study the influence of gallium on amorphous calcium phosphate physicochemical properties, thermal stability, stability in aqueous solution of different compositions, and to investigate antibacterial activity.
2. To evaluate the influence of gallium on the hydroxyapatite physicochemical properties and to determine the optimal gallium concentration in hydroxyapatite to achieve antibacterial properties without causing toxic effects on cells.
3. To investigate the impact of gallium on the thermal stability of hydroxyapatite and to locate possible gallium position in the hydroxyapatite crystal lattice after sintering at different temperatures.

Theses to Defend

1. The addition of gallium delays the crystallisation of amorphous calcium phosphate in various aqueous media and thermally induced crystallisation.
2. Optimal gallium content in the hydroxyapatite can ensure the balance of antibacterial activity and cytocompatibility.
3. Gallium substitutes calcium in the hydroxyapatite lattice, leading to an increase in lattice unit cell volume, affecting the thermal stability and phase composition of hydroxyapatite bioceramics at different sintering temperatures.

Scientific Novelty

The scientific novelty was recognised in the following aspects.

1. For the first time, the influence of gallium on the amorphous calcium phosphate's stability in various aqueous media was studied.
2. The antibacterial activity of gallium containing amorphous calcium phosphate against *S. aureus* was studied.
3. For the first time, the theoretical substitutional structure model of gallium containing hydroxyapatite was developed using *Profex* software and electron density maps.

Practical Significance

The obtained calcium phosphates with enhanced properties such as improved stability, bioactivity, and antibacterial properties could find wide clinical applications, including bone regeneration, implant coatings, and antibacterial biomaterials. Furthermore, understanding the stability of amorphous calcium phosphate will enhance the reliability and longevity of the application. Antibacterial properties provided by gallium addition to the calcium phosphate

biomaterials can reduce antibiotic usage in the bone regeneration field. By reducing the risk of infections in the early stage, improved healing and regeneration will be achieved.

Structure and Volume of the Thesis

This Doctoral Thesis was prepared as a collection of thematically related scientific publications dedicated to gallium containing calcium phosphates. This Thesis unites three original publications and one review article published in international, peer-reviewed, open-access scientific journals indexed in the Science Citation Index (SCI).

Publications and Approbation of the Thesis

The results of the Thesis were published in four SCI scientific publications.

Paper 1: Mosina, M., Kovrlija, I., Stipniece, L., Locs, J., Gallium containing calcium phosphates: Potential antibacterial agents or fictitious truth. *Acta Biomaterialia*, **2022**, *150*, 48–57. https://doi.org/10.1016/j.actbio.2022.07.063 (pen Access, IF 9.6, Q1, CiteScore 17.8).

- The author contributed to the publication by conceptualisation, investigation, visualisation, writing the original draft, reviewing and editing (in total 80/100 %).

Paper 2: Vasiljevs, R., Sceglova, M., Stipniece, L., Locs, J. Insights into physicochemical properties, stability in various aqueous media, and antibacterial activity of gallium-containing amorphous calcium phosphates. *Scientific Reports*, **2025**, *15*, 26976. https://doi.org/10.1038/s41598-025-12906-7 (Open Access, IF 3.9, Q1, CiteScore 6.7).

- The author contributed to the publication through conceptualisation, data curation, formal analysis, reviewing and editing (in total 45/100 %).

Paper 3: Mosina, M., Siverino, C., Stipniece, L., Sceglovs, A., Vasiljevs, R., Moriarty, T. F., Locs, J. Gallium-doped hydroxyapatite shows antibacterial activity against *Pseudomonas aeruginosa* without affecting cell metabolic activity. *J. Funct. Biomater*. **2023**, *14*, 51. https://doi.org/10.3390/jfb14020051 (Open Access, IF 5.2, Q2, CiteScore 6.8).

- The author contributed to the publication through conceptualisation, investigation, data curation, formal analysis, visualisation, writing the original draft, reviewing and editing (in total 70/100 %).

Paper 4: Sceglova, M., Döbelin, N., Vasiljevs, R., Stipniece, L., Locs, J. Influence of gallium doping on the thermal stability and microstructure of sintered hydroxyapatite bioceramics. *Ceramics International* **2025**, *51*(14), 41150–42261. https://doi.org/10.1016/j.ceramint.2025.06.440 (Open Access, IF 5.6, Q1, CiteScore 9.1).

- The author contributed to the publication through conceptualisation, investigation, data curation, formal analysis, visualisation, writing the original draft, reviewing and editing (in total 80/100 %).

The results of the Thesis were presented at 11 scientific conferences.

1. **Mosina, M**., Siverino, C., Stipniece, L., Sceglovs, A., Vasiljevs, R., Moriarty, T. F., Locs, J. Biocompatible gallium doped hydroxyapatite. *Scandinavian Society for Biomaterials*, Jurmala, Latvia, June 2021, online (oral presentation).
2. **Mosina, M**., Siverino, C., Stipniece, L., Sceglovs, A., Vasiljevs, R., Moriarty, T. F., Locs, J. Biocompatible gallium doped hydroxyapatite. *Scandinavian Society for Biomaterials*, Jurmala, Latvia, June 2022 (oral presentation).
3. **Mosina, M**., Siverino, C., Stipniece, L., Sceglovs, A., Vasiljevs, R., Moriarty, T. F., Locs, J. Effect of gallium doped hydroxyapatite on *P.aeruginosa* bacteria growth. *Tissue Engineering and Regenerative Medicine International Society (TERMIS) European Chapter Conference*, Krakow, Poland, July 2022 (oral and poster presentation).
4. **Mosina, M**., Vasiljevs, R., Stipniece, L., Locs, J. Gallium ion effect on calcium phosphate ceramic phase composition. *Bioceramics32*, Venice, Italy, September 2022 (poster presentation).
5. Stipniece, L., **Mosina, M.**, Locs, L., Effect of Gallium on physicochemical characteristics of hydroxyapatite, *3rd Biennial Conference Biomaterials and Novel Technologies for Healthcare* (*BioMaH 2022*), Rome, Italy, October 2022 (poster presentation).
6. Vasiljevs, R., **Mosina, M.**, Crystallization kinetics of gallium-containing amorphous calcium phosphate in different media, *Riga Technical University Student Scientific and Technical Conference*, Riga, Latvia, April 2023 (oral presentation).
7. Vasiljevs, R., **Sceglova, M.**, Stīpniece, L., Ločs, J. Gallium containing amorphous calcium phosphate crystallization kinetics in different media. *Materials Science and Applied Chemistry conference of RTU* (*MSAC 2023*), Riga, Latvia, October 2023 (poster presentation).
8. Vasiljevs, R., **Sceglova, M.**, Stīpniece, L., Ločs, J. Effect of gallium content on crystallization and sinterability of amorphous calcium phosphate. *Riga Technical University Student Scientific and Technical Conference*, Riga, Latvia, April 2024 (oral presentation).
9. Vasiljevs, R., **Sceglova, M**., Stīpniece, L., Ločs, J. Synthesis, characterization and sintering of gallium containing amorphous calcium phosphate. *Riga Technical University Student Scientific and Technical Conference,* Riga, Latvia, April 2025 (oral presentation).
10. **Sceglova, M**., Döbelin, N., Vasiljevs, R., Stipniece, L., Locs, J., Gallium-doped hydroxyapatite and its properties, *The XIXth Conference of the European Ceramic Society* (*ECerS 2025*), Dresden, Germany, September 2025 (poster presentation).
11. Vasiljevs, R., **Sceglova, M**., Stipniece, L., Locs, J. Effect of gallium content on stability and sinterability of amorphous calcium phosphate. *The XIXth Conference of the European Ceramic Society* (*ECerS 2025*), Dresden, Germany, September 2025 (oral and poster presentations).

Other scientific publications published during the development of the Thesis.

1. Stipniece, L., Skadins, I., **Mosina, M**. Silver- and/or titanium-doped β-tricalcium phosphate bioceramic with antibacterial activity against *Staphylococcus aureus*. *Ceramics International*, **2022**, 48(7), 10195–10201. https://doi.org/10.1016/j.ceramint.2021.12.232.
2. Irtiseva, K., **Mosina, M**., Tumilovica, A., Lapkovskis, V., Mironovs, V., Ozolins, J., Stepanova, V., Shishkin, A. Application of granular biocomposites based on homogenised peat for absorption of oil products. *Materials,* **2022**, *15*, 1306. https://doi.org/10.3390/ma15041306.
3. Rezevska, D., Stipniece, L., Rubene, L., **Sceglova, M.**, Maurins, S., Vasiljevs, R., Racenis, K., Kroica, J. Zinc-substituted hydroxyapatite-bacteriophage complexes for complementary antibacterial properties. *Colloids Surf. A*, **2025***, 720*, 137114. https://doi.org/10.1016/j.colsurfa.2025.137114.
4. Sceglovs, A., Siverino, C., Skadins, I., Pirsko, V., Sceglova, M., Kroica, J., Moriarty, F. T., Salma-Ancane, K. Injectable ε-polylysine/hyaluronic acid hydrogels with resistance preventing antibacterial activity for treating wound infections. *ACS Applied Bio Materials,* **2025**, https://doi.org/10.1021/acsabm.5c01252.

MAIN RESULTS OF THE THESIS

GaACP and its Properties (Paper 2)

Syntheses of the ACP powders were performed using a modified wet chemical precipitation method at ambient temperature (20 ± 2 °C). Precipitation of the ACP was induced by the rapid addition of 3M NaOH aqueous solution to an acidic solution containing Ca^{2+} (from $CaCl_2 \cdot 2H_2O$), Ga^{3+} (from $Ga(NO_3)_3 \cdot 9.5H_2O$), and PO_4^{3-} (from H_3PO_4) ions, reaching pH 10.3 ± 0.2. To achieve different Ga contents in the synthesis products, various amounts of $Ga(NO_3)_3 \cdot 9.5H_2O$ were added in the synthesis medium, while the (Ca + Ga)/P (Ca/P for Ga-free ACP) molar ratio of the raw materials was kept constant at 1.67. The sample series were labelled Ref-ACP, 2GaACP, 4GaACP, 6GaACP, and 12GaACP, considering the theoretical Ga content 0 wt%, 2 wt%, 4 wt%, 6 wt%, and 12 wt%, respectively.

The as-synthesised and heat-treated powders were analysed using comprehensive characterisation methods. The phase composition was studied using the X-ray diffraction technique (XRD, *PANalytical Aeris*, The Netherlands), and the crystalline phase identification was done using the PDF-2 database from the International Centre for Diffraction Data (ICDD). The functional groups were analysed using a Fourier transform infrared spectrometer (FTIR, *Nicolet iS 50*, *Thermo Scientific*, USA). The morphology was characterised using a scanning electron microscope (SEM, *Verios 5 UC*, *Thermo Fisher Scientific*, USA) coupled with a scanning transmission electron microscopy (STEM) detector. Specific surface area (SSA_{BET}) of the as-synthesised powders was determined using the *Brunnauer–Emmet–Teller* method (BET) and a QUADRASORB SI instrument (Quantachrome Instruments, USA). True density was determined using a He pycnometer (PYC, *Micro UltraPyc 1200e*, *Quantachrome Instruments*, USA). To evaluate the thermal stability of the as-synthesised powders, thermogravimetric analysis (TGA) combined with differential scanning calorimetry (DSC) was performed using a simultaneous TGA/DSC instrument (TGA/DSC 3+, *Mettler Toledo*, Switzerland).

Regardless of Ga content, all as-synthesised powders were X-ray amorphous, exhibiting a broad diffraction maximum at 30° 2θ, characteristic of ACP (Fig. 2A) [57]–[59].

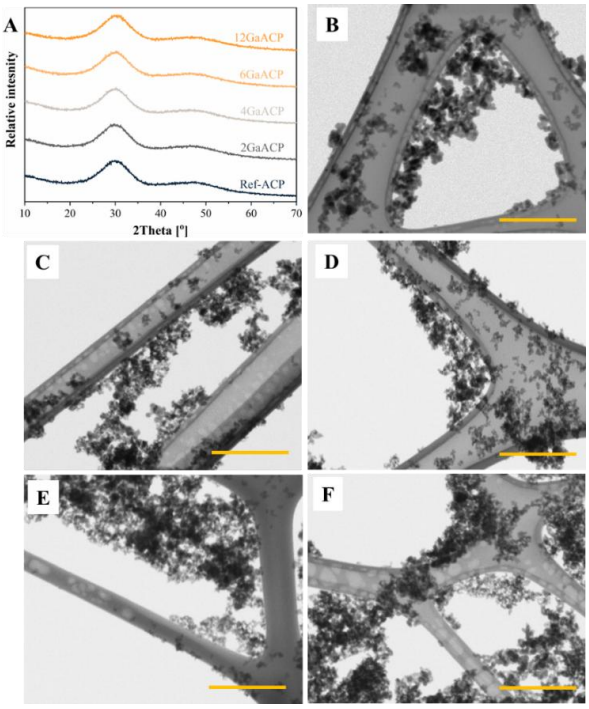

Fig. 2. A – XRD patterns of the Ref-ACP and GaACP powders; STEM microphotographs of B – Ref-ACP, C – 2GaACP, D – 4GaACP, E – 6GaACP, and F –12GaACP powders. Scale bar – 300 nm.

Both the Ref-ACP and GaACP powders had high SSA_{BET} (Table 1), which correlates with available data in the literature [60].

Table 1

Ga content and morphological characteristics of the as-synthesised ACP powders

Sample	Nominal Ga content [wt%]	Measured Ga content [wt%]	SSA_{BET} [m^2/g]	**ρ** [g/cm^3]	d_{BET} [nm]
Ref-ACP	-	-	167 ± 4	2.50 ± 0.02	14 ± 1
2GaACP	2	0.6 ± 0.1	159 ± 5	2.54 ± 0.06	15 ± 1
4GaACP	4	1.3 ± 0.2	151 ± 7	2.49 ± 0.05	16 ± 1
6GaACP	6	1.7 ± 0.1	163 ± 1	2.47 ± 0.02	15 ± 1
12GaACP	12	2.2 ± 0.1	165 ± 18	2.47 ± 0.04	15 ± 2

There is a threshold for Ga incorporation into the ACP structure. The measured content of Ga was significantly lower than nominal values and did not exceed 2 wt% even for samples with the nominal Ga concentration of 6 wt% and 12 wt% (Table 1). ACP exhibits a disordered structure characterised by the absence of long-range crystalline order. ACP particles are composed of randomly arranged *Posner* clusters with an average size of approximately 0.95 nm, which are surrounded by a hydrated layer (up to 25 %) filling in the intercluster space

[61]. The hydrated layer hinders the incorporation of foreign ions, which can explain the limited incorporation of Ga in the ACP. Alternatively, the Ga^{3+} ions that dissociated during the initial synthesis solution may hydrolyse into insoluble hydroxide ($Ga(OH)_3$), which has low bioavailability [46] and does not contribute to the precipitation of GaACP. STEM microphotographs revealed that the Ref-ACP and GaACP powders are composed of nano-sized spheroidal particles (Fig. 2 B–F). The results suggest that Ga does not significantly influence the morphological characteristics of the ACP.

DSC curves show similar thermal effects for both the ACP and the GaACP samples (Fig. 3 A).

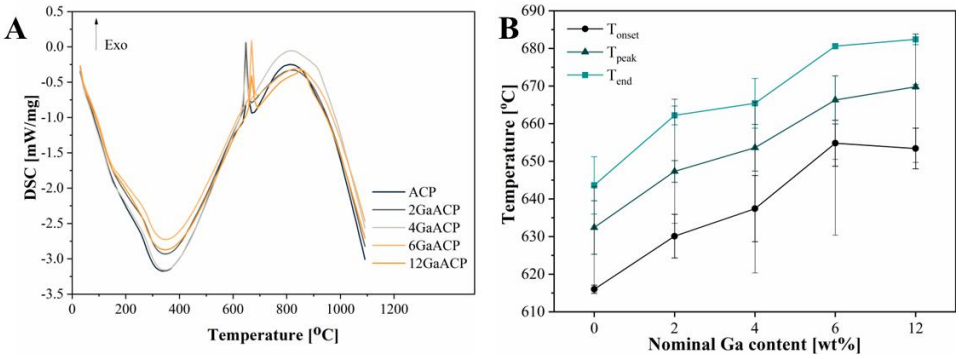

Fig. 3. A – DSC curves of the Ref-ACP and GaACP powders; B – the characteristic phase transition temperatures [unpublished data].

The endothermic peak up to 350 °C corresponds to the release of the free and chemically bonded water and CO_2. This process does not cause the crystallisation of ACP and GaACP. Somrani et al. concluded that water molecules do not directly interact with phosphate groups, and their loss does not change the structure of ACP [62]. An exothermic peak between 615 °C and 680 °C (Fig. 3 A) corresponds to ACP crystallisation into a more stable CaP phase, accompanied by heat release [22], [63]. The addition of Ga improved the thermal stability of ACP; i.e., with increasing Ga content, the crystallisation temperature increased (Fig. 3 B). This observation agrees with the scientific literature, suggesting that the thermal stability of ACP depends on the presence of impurities, namely, stabilising agents (ions or molecules of other metals or non-metals), which contribute to the shift of the phase transition or crystallisation point towards higher temperatures [22], [64]. An additional exothermic effect was observed at 861 °C for the sample with the highest Ga concentration (12GaACP), which could be associated with the crystallisation of the $Ga_x(OH)_yO_z$ cluster. The presence of those clusters was observed by Yang et. al. using NMR analysis [53].

To investigate the thermal stability of the GaACP powders, they were heat-treated at temperatures ranging from 300 °C to 1200 °C, and the phase composition of the heat-treated powders was analysed using XRD patterns (Fig. 4).

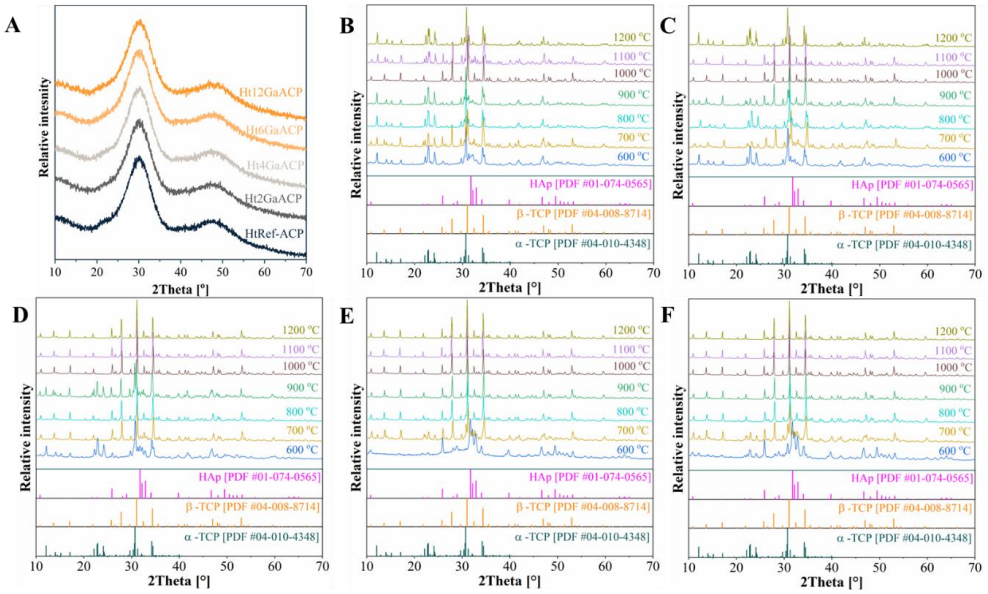

Fig. 4. XRD patterns of the heat-treated powders: A – ACP and GaACP at 300 °C; B – Ref-ACP; C – 2GaACP; D – 4GaACP; E – 6GaACP; F – 12GaACP at 600–1200 °C [unpublished data].

Table 2

Phase composition of the ACP and GaACP powders heat-treated at different temperatures (in each mixture, the phase written first is the major component, i.e., it is present in a higher amount than other phases) [unpublished data]

Temp. [°C]	**Sample series**				
	Ref-ACP	**2GaACP**	**4GaACP**	**6GaACP**	**12GaACP**
300	amorphous	amorphous	amorphous	amorphous	amorphous
600	α-TCP/HAp	α-TCP/HAp/ β-TCP	α-TCP/HAp/ β-TCP	HAp/β-TCP	HAp/α-TCP
700	β-TCP/α-TCP/ HAp	β-TCP/α-TCP/ HAp	β-TCP/HAp/ α-TCP/	β-TCP/α-TCP/ HAp	β-TCP/α-TCP/ HAp
800	α-TCP/β-TCP/ HAp	α-TCP/β-TCP/HAp	β-TCP/α-TCP/ HAp	β-TCP/α-TCP/ HAp	β-TCP/α-TCP/ HAp
900	β-TCP/α-TCP/ HAp	β-TCP/α-TCP/ HAp	α-TCP/β-TCP/HAp	β-TCP/HAp/α-TCP/	β-TCP/HAp
1000	β-TCP/α-TCP/ HAp	β-TCP/α-TCP/ HAp	β-TCP/α-TCP/ HAp	β-TCP/α-TCP/ HAp	β-TCP/α-TCP/ HAp
1100	β-TCP/α-TCP/ HAp	β-TCP/α-TCP	β-TCP/α-TCP/ HAp	β-TCP/HAp	β-TCP/HAp
1200	α-TCP/β-TCP	α-TCP/β-TCP	β-TCP/α-TCP	β-TCP/α-TCP	β-TCP/α-TCP

Regardless of Ga content, the ACP powders remained X-ray amorphous after heat treatment at 300 °C (Fig. 4 A). However, increasing the heat treatment temperature to 600 °C and above induced the formation of various CaP phases (Fig. 4 B–F). The phase composition of the heat-

treated powders was a mixture of two or three phases compromising α-TCP, β-TCP, and HAp in different ratios (Table 2).

Usually, α-TCP or β-TCP is formed from ACP after heat treatment at temperatures above 600 °C, as the ACP Ca/P molar ratio is 1.5, which corresponds to TCP [65]. However, in our study, we observed the formation of the HAp phase. This is explained by the synthesis conditions, namely, a higher Ca/P molar ratio (Ca + Ga/P = 1.67 and Ca/P = 1.67) in the synthesis medium, and the possible presence of carbonate ions (incorporating or substituting phosphate groups) into the structure of the as-synthesised Ref-ACP and GaACP. The carbonate ions leave the ACP structure during heat treatment, increasing the Ca/P molar ratio, thus promoting the formation of HAp [66]. Nevertheless, there is no correlation between Ga content, temperature and phase composition of the final products after heat treatment. ACP atomic arrangement is inherently disordered and non-uniform, resulting in unpredictable phase composition after heat treatment.

Due to the metastable nature of ACP in aqueous media, it is important to evaluate its behaviour under *in vitro* experimental conditions. Different factors, such as pH, ionic doping, and additives, affect ACP stability in aqueous media. The elucidation of stability will help to understand material behaviours and optimise material formulations for specific biomedical environments and applications.

Ga's influence on the stability of ACP in aqueous media

The stability of GaACP powder was evaluated in deionised water (DI H_2O), phosphate buffer solution (PBS), Dulbecco's modified Eagle's medium (DMEM) and tryptic soy broth (TSB). The powder and liquid media ratio was 6 mg/L. Samples were incubated at 37 °C with orbital shaking at 80 rpm for 20 min, 40 min, 60 min, and 90 min, and 4 h, 24 h, and 48 h. The stability time of powders in different aqueous media is summarised in Fig. 5 A.

In vitro stability of the powders was evaluated by XRD, where the formation and narrowing of diffraction maxima characteristic of the apatitic CaP phase at 26^o and 32^o 2θ was observed (Fig. 5B-F) [67]. Rapid crystallisation of ACP in PBS regardless of Ga content was observed. It is related to the presence of phosphate ions in the media, which accelerates the nucleation and precipitation of new particles following a dissolution-recrystallisation mechanism [68]–[70]. The significant effect of Ga on the ACP stability was observed in DI H_2O, DMEM (Fig. 5 B–F), and TSB. In DMEM, the stability of the ACP increased gradually with the Ga content. DMEM was buffered with $NaHCO_3$, thus supplementing the media with carbonate ions or causing precipitation of calcite, which, in turn, can contribute to the stabilisation of ACP [22], [64], [71], [72].

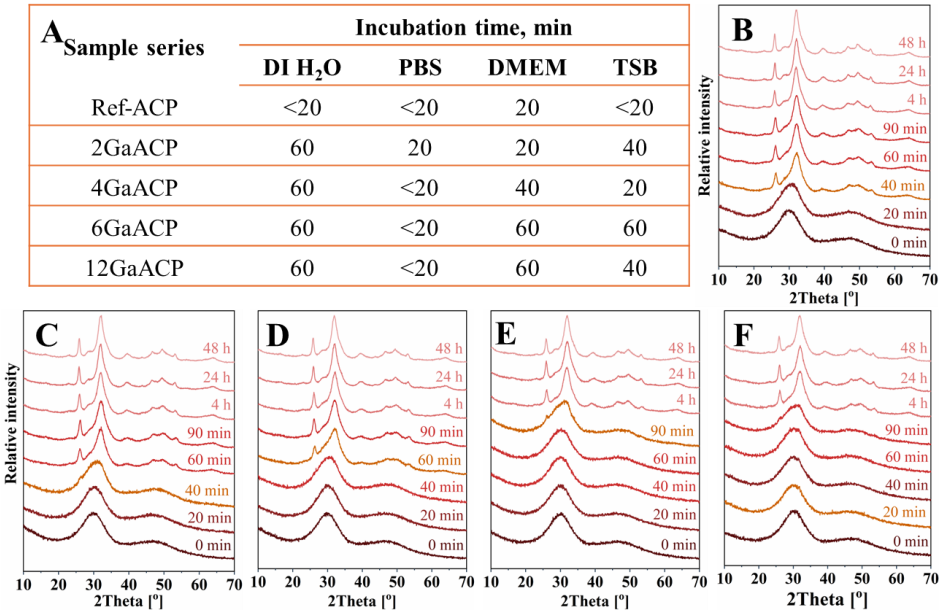

A Sample series	Incubation time, min			
	DI H_2O	PBS	DMEM	TSB
Ref-ACP	<20	<20	20	<20
2GaACP	60	20	20	40
4GaACP	60	<20	40	20
6GaACP	60	<20	60	60
12GaACP	60	<20	60	40

Fig. 5. A – Stability time of the Ref-ACP and GaACP powders in different aqueous media. XRD patterns after incubation in DMEM: B – Ref-ACP, C – 2GaACP, D – 4GaACP, E – 6GaACP, and F – 12GaACP [Paper 2].

Additionally, in the literature, there is evidence that organic molecules stabilise the ACP phase. Still, it depends on the type of organic molecules and their concentration [73]–[75]. Both TSB and DMEM contain amino acids, vitamins and proteins, which can be adsorbed onto the surface of the ACP nanoparticle, thereby stabilising them. The stability tests revealed that not only does Ga ion influence the stability, but also the composition of the media.

After understanding ACP performance in the *in vitro* media, the next step is to evaluate antibacterial activity. It is known that Ga possesses antibacterial properties. Moreover, Yang et al. revealed that GaACP has an inhibitory effect on the growth of *P. aeruginosa* [53]. However, it is important to evaluate the potential inhibition effect also against *S. aureus*, as it is a major contributor to infections associated with biomaterials, especially in orthopaedic surgeries.

Evaluation of GaACP antibacterial activity

Antibacterial properties were assessed against *P. aeruginosa* (ATCC 23863) and *S. aureus* (ATCC 25923) by measuring optical density at 620 nm (OD_{620}) of bacterial growth for 20 h at 37 °C in TSB by using a spectrophotometer (*MultiskanFC, Thermo Scientific*, USA) (Fig. 6).

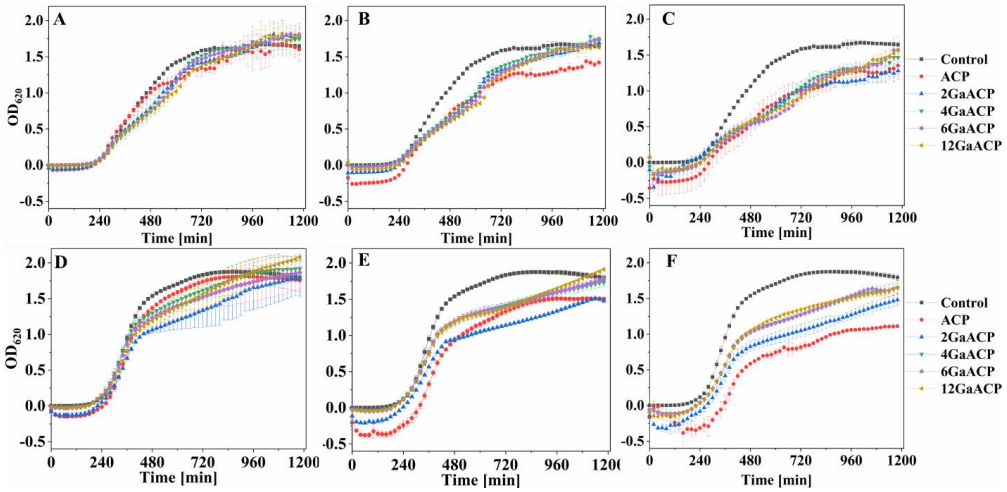

Fig. 6. *P. aeruginosa* growth kinetic curves in the presence of the GaACP powder suspensions in TSB at: A – 1 mg/mL, B – 2 mg/mL, and C – 4 mg/mL. *S. aureus* growth kinetic curves in the presence of the GaACP powder suspensions in TSB media at: D – 1 mg/mL, E – 2 mg/mL, and F – 4 mg/mL. The represented OD_{620} values were obtained by subtracting the initial $OD_{620\text{-}0\_h}$ (starting time = 0 h) from the measured $OD_{620\text{-}x\_h}$ at specific time points, i.e., x h.

No significant differences in the *P. aueruginosa* and *S. aureus* bacteria growth curves were observed for the ACP and GaACP powders at 1 mg/mL concentration in TSB. By increasing powder concentration to 2 mg/mL, the delayed exponential growth (log phase) compared to the control was observed against both bacterial strains. At the powder concentration of 4 mg/mL, the inhibitory effect became more pronounced and differed between bacterial strains. In the case of *S. aureus*, at a powder concentration of 4 mg/mL, the ACP and GaACP showed similar bacterial growth inhibition effects. A more pronounced impact of Ga content was noted in the *P. aeruginosa* culture, which lacked a distinct log phase (exponential) and could not achieve a stationary phase. Thus, the bacteriostatic effect of Ga was indirectly revealed. However, this effect can also be related to the nanosized ACP and GaACP particles, which can adversely affect bacteria by damaging cell membranes, hindering DNA synthesis, and interfering with metabolic functions [76]–[78]. Additionally, bacteria grow exponentially in the presence of other CaP phases, non-amorphous, as from stability studies (Fig. 5 A). After 40 min, all samples converted to a more stable CaP phase, Ca-deficient HAp (CDHAp). It is still unclear whether Ga^{3+} ions are being released into the solution during this process or are incorporated into the crystal structure of CDHAp.

The first objective of the research was successfully achieved, demonstrating that Ga does not influence the physicochemical properties of the ACP powder, while the presence of Ga affected the stability of ACP. The GaACP powders did not show sufficient antibacterial activity for potential use in treating infection. Accordingly, research was conducted to determine how Ga affects HAp, where potentially higher Ga incorporation levels and antibacterial activity could be achieved.

GaHAp and its Properties (Paper 3)

The HAp powders with different Ga content (Fig. 7 A) and (Ca + Ga)/P (Ca/P for Ga-free HAp) molar ratio of 1.67 were synthesised via the wet chemical precipitation method from calcium oxide (CaO), gallium nitrate hydrate ($Ga(NO_3)_3 \cdot 9.5H_2O$) and phosphoric acid (H_3PO_4). 2M H_3PO_4 aqueous solution was added to the Ca^{2+} and Ga^{3+} ions containing suspension with a 1 mL/min addition rate, continuous stirring at 150 rmp until the pH 6.90 ± 0.05 at 45 °C was reached. The obtained precipitates were aged overnight in the mother liquors, vacuum-filtered and dried at 105 °C (overnight). The as-synthesised samples were labelled as HAp, 2GaHAp, 4GaHAp, 6.3GaHAp, and 8GaHAp and characterised with multiple analysis techniques (XRD, FTIR, BET) described above in section "GaACP and its Properties (Paper 2)". *In vitro* Ga^{3+} ion release tests were performed in DMEM for GaHAp paste (non-dried sample, filtered precipitates) for up to 30 days.

Low-intensity maxima characteristic of low-crystalline apatite were detected in the XRD patterns of all samples (Fig. 7 B). The addition of Ga reduced particle size and increased SSA_{BET} compared to Ga-free HAp (Fig. 7 A), suggesting that Ga inhibits HAp crystal growth. The adsorption of smaller ions, such as Ga^{3+} (0.62 Å [79]) compared to Ca^{2+} (1.00 Å [79]), on the HAp crystal surface results in the inhibition of crystallisation and crystal growth as suggested in the literature [54], [55], [80], [81].

A Sample	Theoretical Ga content [wt%]	Gallium content [wt%]	SSA_{BET} [m^2/g]	ρ [g/cm^3]	d_{BET} [nm]
HAp	-	-	71 ± 7	2.77 ± 0.04	31 ± 3
2GaHAp	2	1.6 ± 0.1	95 ± 5	2.85 ± 0.06	22 ± 1
4GaHAp	4	3.3 ± 0.4	117 ± 4	2.80 ± 0.06	18 ± 1
6.3GaHAp	6.3	5.5 ± 0.1	109 ± 2	2.83 ± 0.01	20 ± 1
8GaHAp	8	6.9 ± 0.5	102 ± 5	2.79 ± 0.03	21 ± 1

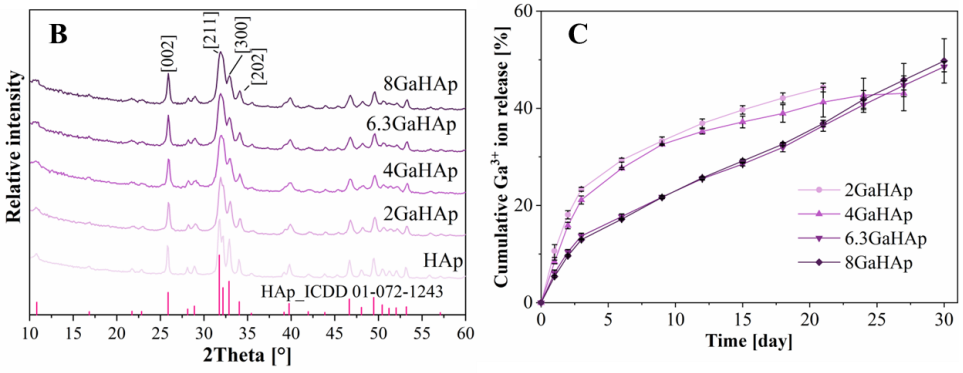

Fig. 7. A – Physicochemical parameters of the as-synthesised HAp and GaHAp powders; B – XRD patterns of the as-synthesised HAp and GaHAp powders; C – cumulative Ga^{3+} ion release in DMEM media at 37 °C (n = 3 ± SD) [82].

Due to this effect, it cannot be ruled out that the synthesised HAp powders may contain amorphous phase impurities. Furthermore, increasing of the Ga content resulted in a decrease

in the Ca/P molar ratio in the final products. Thus, it can be claimed that the obtained products are non-stoichiometric HAp or CDHAp. The results of *in vitro* Ga^{3+} ion release tests (Fig. 7 C) demonstrated the potential for long-term antibacterial ion delivery, with up to 43 % of Ga released into the media over 27 days.

***In vitro* evaluation of GaHAp**

The antibacterial properties of the GaHAp powders were analysed by assessing the growth of five different bacterial cultures – *P. aeruginosa* (Paer09), *E. coli* (ATCC 25922), *S. epidermidis* (ATCC 35984), *S. aureus* (JAR 06013), and *Streptococcus pyogenes (S. pyogenes,* ATCC 19615) at 37 °C for 18 h by measuring the optical density at 600 nm (OD_{600}) using a spectrophotometer (*MultiskanGo; Thermo Scientific*, USA).

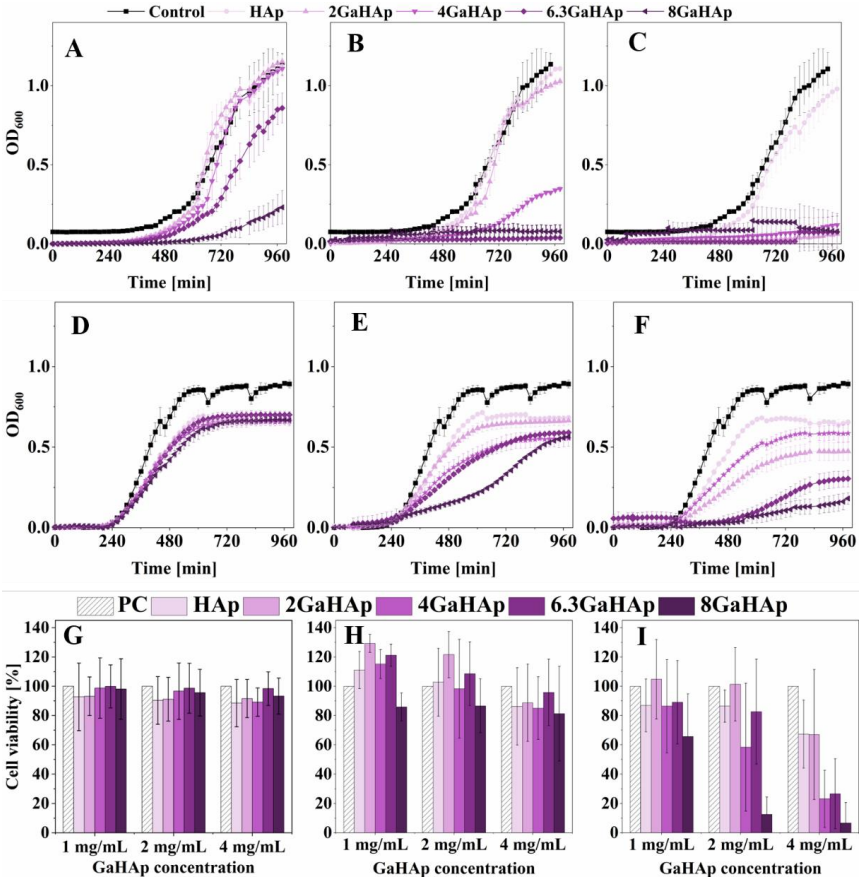

Fig. 8. The GaHAp powder suspension induced growth inhibition of *P. aeruginosa* at concentrations of: A – 1 mg/mL, B – 2 mg/mL, C – 4 mg/mL, and *S. aureus* at concentrations of: D – 1 mg/mL, E – 2 mg/mL, F – 4 mg/mL. Metabolic activity of human fibroblasts (hTERT-BJ1) exposed to the GaHAp powder suspensions at different concentrations (1 mg/mL, 2 mg/mL, and 4 mg/mL) obtained using the direct test: G – day 1, H – day 3, and C – day 7 (PC – positive control).

The bacterial growth kinetics in the GaHAp powders' suspensions at concentrations of 1 mg/mL, 2 mg/mL, and 4 mg/mL were investigated in TSB. Cytotoxicity of the GaHAp powders was tested on telomerase-immortalised human foreskin fibroblasts (hTERT BJ1) cultivated in DMEM via direct tests of the GaHAp powders (at concentrations of 1 mg/mL, 2 mg/mL, and 4 mg/mL in DMEM) and indirect tests of the GaHAp pastes (250 ± 50 mg) up to 7 days [82].

The GaHAp powders exhibited bacteriostatic effect against all five tested bacteria; however, the most pronounced inhibition was observed against *P. aeruginosa* (Fig. 8 A–C), as *P. aeruginosa* has an iron-dependent metabolism, which is disrupted by Ga^{3+} ions [51].

The *P. aeruginosa* growth inhibition was observed at 1 mg/mL concentration for the 6.3GaHAp and 8GaHAp powders, which was not observed for *S. aureus* (Fig. 8 D–F). Whereas inhibition of orthopaedic infection-related bacteria, *S. aureus* and *S. epidermidis*, was detected at 2 mg/mL and 4 mg/mL concentrations of the 4GaHAp, 6.3GaHAp, and 8GaHAp powders. Notably, this bacterial inhibition occurred at higher GaHAp powder concentrations than reported in the literature. For instance, Kurtjak et al. observed inhibition of *P. aeruginosa* growth with 0.9 g/mL GaHAp containing 3 wt% of Ga [54]. In addition, Ballardini et al. showed the antibacterial effect of the GaHAp with Ga content 1 wt%, where bacterial reduction of *P. aeruginosa* and *S. aureus* after 24 h was above 80 % [83]. Even though in all the mentioned studies, the analysed substance was GaHAp, the findings indicate that the synthesis method and parameters significantly influences the incorporation of Ga and key properties of the final material.

To evaluate cytotoxicity, hTERT-BJ1 fibroblast cells were directly exposed to the GaHAp powder suspensions in DMEM at the same concentrations as in the antibacterial tests (1 mg/mL, 2 mg/mL, and 4 mg/mL) (Fig. 8 G–I). After three days, metabolic activity remained above 80 %. However, by day 7, cell viability sharply reduced below 40 % for all the Ga-containing samples at 2 mg/mL and 4 mg/mL, highlighting the importance of optimising Ga^{3+} concentration for biocompatibility. The indirect tests assessed the impact of ions released from the GaHAp paste into the cell media on the chosen cell line (Fig. 9 A).

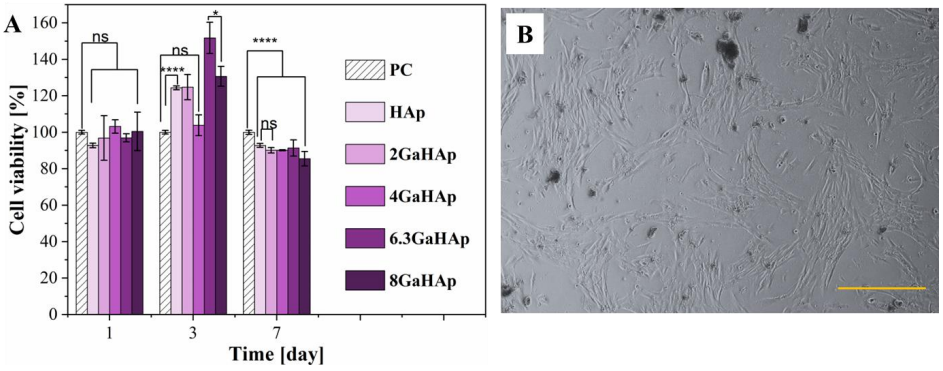

Fig. 9. A – Metabolic activity of human fibroblasts exposed to the GaHAp pastes via indirect test; B – microscope images of human fibroblasts after the indirect test on day 3. Scale bar 200 μm.

Results indicated no cytotoxic effects, as cell viability remained around 90 %. Notably, samples with Ga content of 5.5 ± 0.1 wt% and 6.9 ± 0.5 wt% significantly enhanced metabolic activity on day 3 and day 7, suggesting that both Ga^{3+} and Ca^{2+} ions have a stimulatory effect on the cells.

The results of the research show the importance of evaluating the influence of Ga on the as-synthesised HAp and the interactions between the developed biomaterial and cells. Obtained GaHAp powders showed advantageous properties for the early-stage treatment of bone defects compared to the studied GaACP powders. Moreover, regarding the toxicity evaluation of the GaHAp powders, an adverse effect towards human fibroblasts was not observed. It was concluded that the GaHAp could prevent the development of chronic and acute infections due to the bacteriostatic effect on both gram-positive and gram-negative bacterial species. Accordingly, in the next study, the bioceramics were developed using the 2GaHAp (1.6 ± 0.1 wt% of Ga) and 4GaHAp (3.3 ± 0.4 wt% of Ga) powders. The compositions were chosen since the respective Ga concentrations provided both antibacterial activity and did not show a toxic effect on the cells.

GaHAp Bioceramics (Paper 4)

GaHAp bioceramics were prepared by uniaxially compacting the as-synthesised GaHAp precursor powders at 100 MPa for 1 min, followed by high-temperature sintering in the range from 600 °C to 1200 °C. The phase composition and the theoretical Ga substitution position in the HAp structure of heat-treated powders were analysed using XRD and Rietveld refinement by *Profex* software. The apparent density of the sintered bioceramics was determined using Archimedes principle and a density determination kit (*YDK 01*, *Sartorius AG*, Germany). The microstructure of the bioceramics was characterised using SEM.

Phase composition analysis revealed the formation of a secondary α-TCP phase above 800 °C (Fig. 10 A–C). The content of the secondary phase increased with increasing Ga concentration (Fig. 10 D).

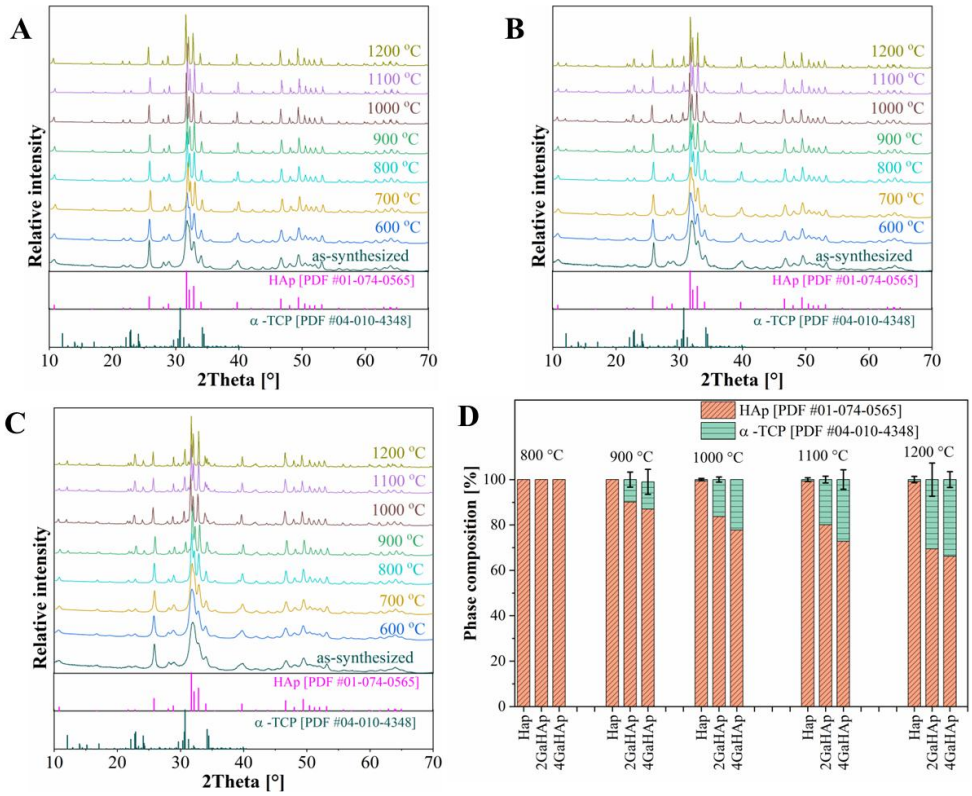

Fig. 10. XRD patterns of the heat-treated A – HAp, B – 2GaHAp, and C – 4GaHAp powders. D – Phase compositions of the samples.

As discussed previously, the as-synthesised powders were CDHAp with Ca/P < 1.67 and with the impurities of an amorphous phase. A combination of these two main characteristics of precursor powder leads to the formation of low-temperature α-TCP at ≥ 900 °C, even though the stability of α-TCP is reported to be in the range of 1120–1430 °C [84], [85]. The presence of the secondary phase (α-TCP) can potentially improve the biodegradability of HAp

bioceramics. Namely, the presence of more soluble α-TCP phase could increase the solubility of the bioceramics, providing improved ion release and bioactivity [42].

The ATR-FTIR spectra (Fig. 11 A–C) exhibited characteristic CaPs' PO_4^{3-}, OH^-, CO_3^{2-}, and HPO_4^{2-} groups' absorbance bands.

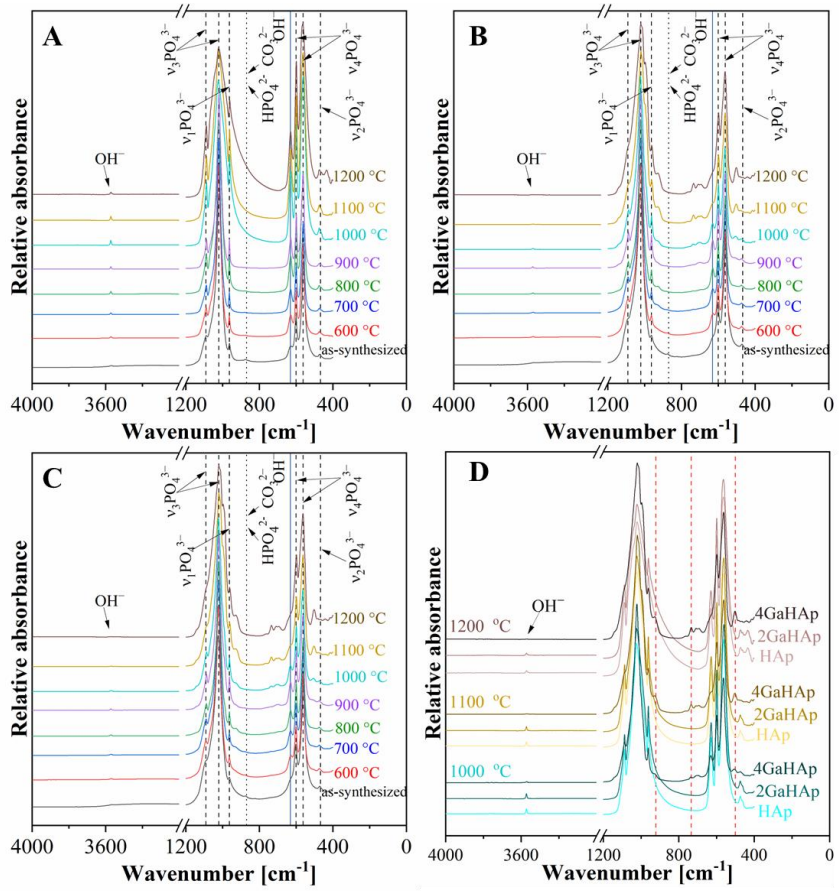

Fig. 11. ATR-FTIR spectra of A – HAp, B – 2GaHAp, and C – 4GaHAp powders heat-treated at temperatures ranging from 600 °C to 1200 ºC. D – extra functional group maxima (marked with red lines) for samples heat-treated at 1000 °C, 1100 °C and 1200 ºC.

Due to cationic deficiency, charge compensation was maintained by substituting HPO_4^{2-} for PO_4^{3-}. Absorbance bands of CO_3^{2-} and HPO_4^{2-} disappeared after heat treatment [87]. Furthermore, a decrease in the absorbance of OH^- groups approximately at 3600 cm^{-1} was observed, which is related to the presence of the secondary phase. The presence of secondary phase also affected PO_4^{3-} groups after heat treatment at 900–1000 °C. Additional absorbance bands were detected as "shoulders", which became more pronounced as the heat treatment temperature increased. In the case of 2GaHAp and 4GaHAp powders heat-treated above 1000 °C, extra absorbance bands at 502 cm^{-1}, 734 cm^{-1}, and 928 cm^{-1} were detected, and the intensity of these bands increased with increasing Ga content. It is difficult to reach definitive

conclusions about forming new functional groups due to the overlapping of the absorbance bands from various phases and impurities in the same spectral area. However, the identified absorbance bands could be related to the potential development of Ga-O bonds. According to existing literature, Ga_2O_3 heat-treated at 1000 °C exhibits bands (duplicates) within the 400–850 cm^{-1} range [46], which aligns with the area indicating the formation of the detected new groups.

Theoretical Ga substitution in the HAp crystal lattice

To locate Ga substitution in the HAp crystal lattice and observe lattice changes prompted by substitution, a complete structure Rietveld refinement of the sample was performed. From the refinement results, the refined unit cell volume of the HAp and GaHAp heat-treated at 1000 °C, 1100 °C, and 1200 °C was calculated and displayed in Fig. 12 A. The results showed that the unit cell volumes of HAp increased with increasing Ga content, suggesting that Ga^{3+} ions are incorporated into the HAp crystal lattice.

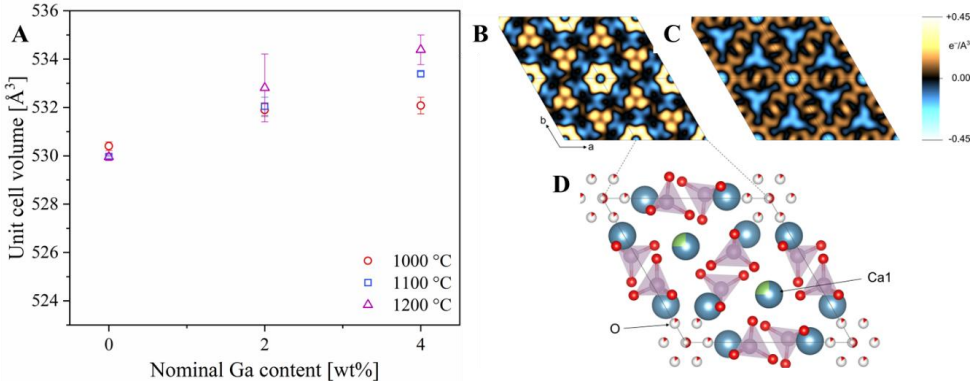

Fig. 12. A – Refined unit cell volume of the HAp and GaHAp heat-treated at 1000 °C, 1100 °C, and 1200 °C as a function of the nominal Ga concentration; F_{obs}–F_{calc} Fourier synthesis maps at z = 0.0 of the 4GaHAp heat-treated at 1100 °C refined B – without and C – with the substitution model for Ga. The model is depicted schematically in D – "O" marks the additional oxygen ion compensating the charge imbalance introduced by Ga incorporation on "Ca1".

The theoretical substitution model was created based on the full structural refinement of the 4GaHAp heat-treated at 1100 °C, including refinement of Ca site occupancy factors, fractional coordinates, and thermal displacement parameters. Firstly, different Fourier maps of the refined structure were created with the Electron Density Map module in *Profex*. Structure refinement of the hexagonal HAp phase in the dataset 4GaHAp heat-treated at 1100 °C with a Ga-free hexagonal structure model, showed residual unfitted electron densities at the Ca1 position (Fig. 12 B). In addition, along the *c*-axis hosting the OH^- groups, formation of the excess electron densities in the form of a hexagonal "flower" was observed (Fig. 12 B). By suggesting and creating a structural model where Ca1 was a partial substitution for Ga^{3+} and charge imbalance was compensated by an additional O^{2-} ion in the OH^- channels, the F_{obs}–F_{calc} Fourier synthesis maps revealed no excess or residual electrons, and the structure remained neutral

(Fig. 12 C). This explains the expansion of the crystalline unit cell volume, where additional incorporation of oxygen ions in the channel compensates for the additional positive charge introduced by Ga^{3+} substitution in the Ca1 site. The substitution model reveals the formation of a defect in the lattice that further affects the microstructure of the bioceramic.

Microstructure of GaHAp bioceramics

Lattice structural and phase composition changes induced by Ga incorporation significantly influenced HAp bioceramics' sinterability, causing a notable decrease in apparent density (Fig. 13 A) and the shrinkage (Fig. 13 B). Additionally, SEM micrographs (Fig. 14 A–I) showed micropore formation, as a formation of secondary phase occurred during sintering, which inhibits densification of bioceramics. It can be explained by the effect of secondary phase particles on grain boundary motion, as at intermediate temperatures during the sintering process, CDHAp converts to α-TCP, which limits grain boundary motion. At the same time, HAp continues to function as the matrix, and secondary phases generate dispersed particles at the grain boundaries that hinder grain growth [88].

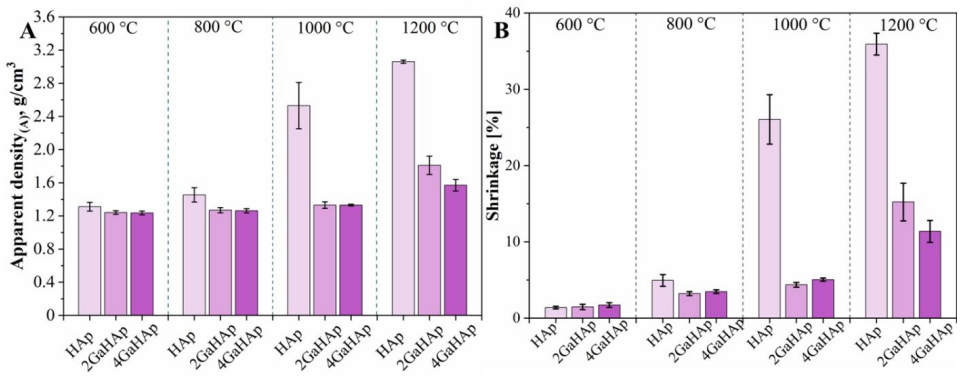

Fig. 13. A – Apparent density and B – shrinkage of the HAp and GaHAp bioceramics after sintering at 600 °C, 800 °C, 1000 °C, and 1200 °C.

SEM micrographs revealed that increasing the sintering temperature led to increased grain sizes. Ga incorporation promoted the formation of smaller grains. In the case of the HAp bioceramics, characteristic hexagonal grains formed above 1000 ^{o}C (Fig. 14 G, J, M). However, for the GaHAp bioceramics, formation of characteristic hexagonal grains was observed at a 1200 ^{o}C sintering temperature.

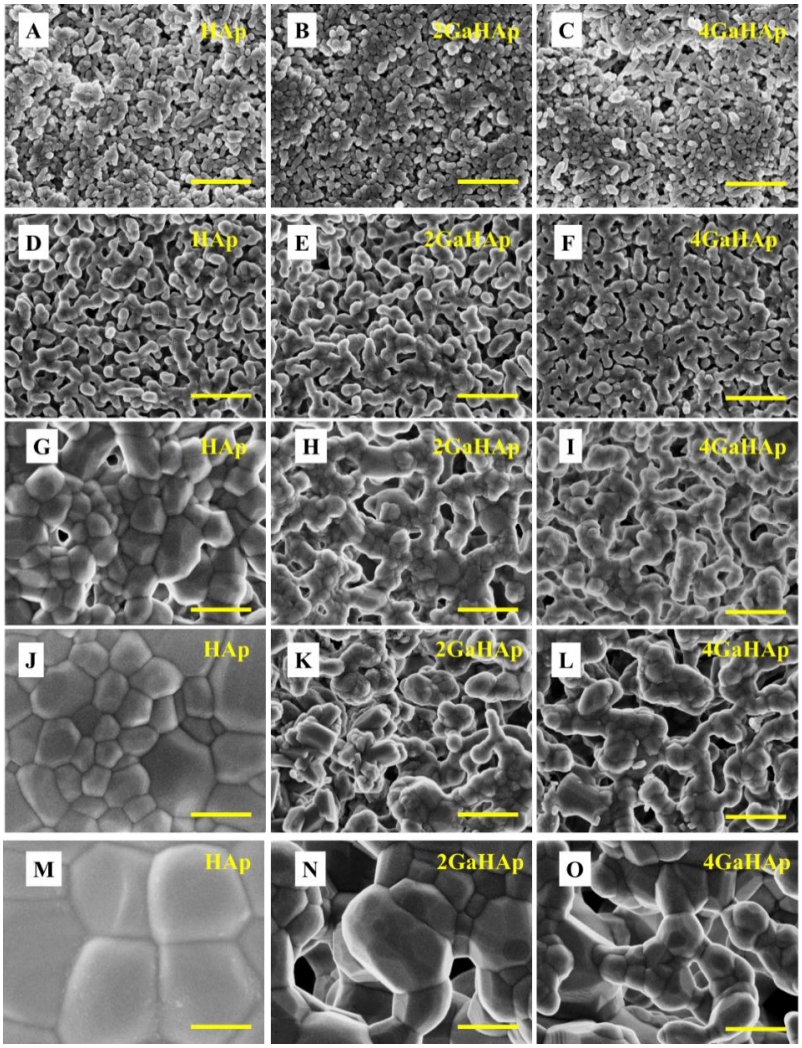

Fig. 14. SEM microphotographs of the A – HAp, B – 2GaHAp, and C – 4GaHAp bioceramic pellets sintered at 600 °C, the D – HAp, E – 2GaHAp, F – 4GaHAp bioceramic pellets sintered at 800 °C, the G – HAp, H – 2GaHAp, and I – 4GaHAp bioceramic pellets sintered at 1000 °C, the J – HAp, K – 2GaHAp, L– 4GaHAp bioceramic pellets sintered at 1100 °C, and the M – HAp, N – 2GaHAp, and O – 4GaHAp bioceramic pellets sintered at 1200 °C. Scale bar – 500 nm [89].

The in-depth substitution behaviour of Ga in the HAp crystal lattice was explored to gain deeper insight into the properties of GaHAp bioceramics. The results demonstrated that partial Ca substitution with Ga can significantly change the HAp thermal behaviour.

CONCLUSIONS

1. Incorporation of gallium in amorphous calcium phosphate is limited to 2.2 ± 0.1 wt% and does not have a significant effect on its physicochemical properties. However, gallium improves the stability of amorphous calcium phosphate in deionised H_2O and in biologically relevant media, i.e., Dulbecco's modified Eagle's medium and tryptic soy broth.
2. Amorphous calcium phosphate and gallium-containing amorphous calcium phosphate powders at a concentration of 4 mg/mL show bacteriostatic effect against *Pseudomonas aeruginosa* and *Staphylococcus aureus*.
3. Gallium inhibits the crystal growth of hydroxyapatite, resulting in a decrease in crystallinity and the formation of smaller particles. The low-crystalline gallium-containing hydroxyapatite provides long-term gallium ion release up to 28 days.
4. The optimal gallium content in hydroxyapatite is in the range from 2 wt% to 5.5 ± 0.1 wt%, providing bacteriostatic effect against *Pseudomonas aeruginosa* and *Staphylococcus aureus* without substantial toxicity towards human fibroblasts.
5. The addition of gallium affects the physicochemical properties of hydroxyapatite precursor powders, leading to the formation of biphasic bioceramics consisting of hydroxyapatite and tricalcium phosphate after heat treatment of hydroxyapatite at temperatures above 900 °C. The secondary phase and lattice defects promote the formation of a microporous structure of the bioceramics and decrease shrinkage.
6. Gallium in the hydroxyapatite crystal lattice occupies the Ca1 position and creates vacancies in the OH^- channels. Charge compensation is achieved by an uptake of O^-, which leads to unit cell volume expansion.

REFERENCES

1. J. M. Wallace, Skeletal Hard Tissue Biomechanics. In D. B. Burr, M. R. Allen, editors. Basic and Applied Bone Biology. Academic Press; 2019, 125–140. https://doi.org/10.1016/B978-0-12-813259-3.00007-5.

2. D. L. Stocum, Regeneration of Musculoskeletal Tissues. In D. L. Stocum, editor. Regenerative Biology and Medicine. Academic Press, 2012, 127–160. https://doi.org/10.1016/B978-0-12-384860-4.00006-X.

3. W. Jiang, H. Liu, Nanocomposites for bone repair and osteointegration with soft tissues. In H. Lui, editor. Nanocomposites for Musculoskeletal Tissue Regeneration. Woodhead Publishing, 2016, 241–257. https://doi.org/10.1016/B978-1-78242-452-9.00011-X.

4. A. H. Hoveidaei, M. Sadat-Shojai, S. Mosalamiaghili, S. R. Salarikia, H. Roghani-shahraki, R. Ghaderpanah, M. H. Ersi, J. D. Conway, Nano-hydroxyapatite structures for bone regenerative medicine: Cell-material interaction. Bone. 179 (2024) 116956. https://doi.org/10.1016/j.bone.2023.116956.

5. I. Roohani, S. Cheong, A. Wang, How to build a bone? – Hydroxyapatite or Posner's clusters as bone minerals. Open Ceramics. 6 (2021) 100092. https://doi.org/10.1016/J.OCERAM.2021.100092.

6. A. Lotsari, A. K. Rajasekharan, M. Halvarsson, M. Andersson, Transformation of amorphous calcium phosphate to bone-like apatite. Nat. Commun. 9 (2018) 4170. https://doi.org/10.1038/s41467-018-06570-x.

7. F. Nudelman, P. H. H. Bomans, A. George, G. de With, N. A. J. M. Sommerdijk, The role of the amorphous phase on the biomimetic mineralization of collagen, Faraday Discuss. 159 (2012) 357-370. https://doi.org/10.1039/c2fd20062g.

8. S. T. J. Tsang, A. J. van Rensburg, J. van Heerden, G. Z. Epstein, R. Venter, N. Ferreira, The management of critical bone defects: outcomes of a systematic approach, European Journal of Orthopaedic Surgery and Traumatology. 34 (2024) 3225–3231. https://doi.org/10.1007/S00590-024-04050-1.

9. A. Díaz-Cuenca, D. Rabadjieva, K. Sezanova, R. Gergulova, R. Ilieva, S. Tepavitcharova, Biocompatible calcium phosphate-based ceramics and composites, Mater Today Proc. 61 (2022) 1217–1225. https://doi.org/10.1016/J.MATPR.2022.01.329.

10. M. C. Schulz, S. Holtzhausen, B. Nies, S. Heinemann, D. Muallah, L. Kroschwald, K. Paetzold-Byhain, G. Lauer, P. Sembdner, Three-Dimensional Plotted Calcium Phosphate Scaffolds for Bone Defect Augmentation – A New Method for Regeneration, Journal of Personalized Medicine. (2023) 13(3) 464. https://doi.org/10.3390/JPM13030464.

11. A. B. G. de Carvalho, M. Rahimnejad, R. L. M. S. Oliveira, P. Sikder, G. S. F. A. Saavedra, S. B. Bhaduri, D. Gawlitta, J. Malda, D. Kaigler, E. S. Trichês, M. C. Bottino, Personalized bioceramic grafts for craniomaxillofacial bone regeneration, International Journal of Oral Science 16 (2024) 63. https://doi.org/10.1038/s41368-024-00327-7.

12. M. Bohner, Resorbable biomaterials as bone graft substitutes, Materials Today. 13(1–2) (2010) 24–30. https://doi.org/10.1016/S1369-7021(10)70014-6.

13. M. Bohner, Calcium orthophosphates in medicine: from ceramics to calcium phosphate cements, Injury. 31 (2000) D37–D47. https://doi.org/10.1016/S0020-1383(00)80022-4.

14. T. Lu, L. Zhang, X. Yuan, J. Ye, A novel calcium phosphate-based ceramic scaffolds with unexpected high osteogenic activity by strontium doping, Mater Today Chem. 36 (2024) 101931. https://doi.org/10.1016/J.MTCHEM.2024.101931.

15. J. A. da Cruz, R. R. Pezarini, A. J. M. Sales, S. R. Benjamin, P. M. de Oliveira Silva, M. P. F. Graça, Study of biphasic calcium phosphate (BCP) ceramics of tilapia fish bones by age, Spectrochim., Acta A Mol. Biomol. Spectrosc. 316 (2024) 124289. https://doi.org/10.1016/J.SAA.2024.124289.

16. A. K. Rajendran, M. S. J. Anthraper, N. S. Hwang, J. Rangasamy, Osteogenesis and angiogenesis promoting bioactive ceramics, Materials Science and Engineering: R: Reports. 159 (2024) 100801. https://doi.org/10.1016/J.MSER.2024.100801.

17. V. I. dos Santos, J. Chevalier, M. C. Fredel, B. Henriques, L. Gremillard, Ceramics and ceramic composites for biomedical engineering applications via Direct Ink Writing: Overall scenario, advances in the improvement of mechanical and biological properties and innovations, Materials Science and Engineering: R: Reports. 161 (2024) 100841. https://doi.org/10.1016/J.MSER.2024.100841.

18. C. Liu, C. Shao, L. Zhang, Q. Huang, Biomaterials and MSCs composites in regenerative medicine, Mesenchymal Stem Cells: Biological Concepts, Current Advances, Opportunities and Challenges. (2023) 69–99. https://doi.org/10.1016/B978-0-323-95346-7.00004-X.

19. S. Thomas, B. S. P. Harshita, P. Mishra, S. Talegaonkar, Ceramic Nanoparticles: Fabrication Methods and Applications in Drug Delivery, Curr. Pharm. Des. 21(42) (2015) 6165–6188. https://doi.org/10.2174/1381612821666151027153246.

20. S. V. Dorozhkin, Synthetic amorphous calcium phosphates (ACPs): preparation, structure, properties, and biomedical applications, Biomater. Sci. 9 (2021) 7748–7798. https://doi.org/10.1039/D1BM01239H.

21. X. Hou, L. Zhang, Z. Zhou, X. Luo, T. Wang, X. Zhao, B. Lu, F. Chen, L. Zheng, Calcium Phosphate-Based Biomaterials for Bone Repair, Journal of Functional Biomaterials. 13 (2022) 187. https://doi.org/10.3390/JFB13040187.

22. C. Combes, C. Rey, Amorphous calcium phosphates: Synthesis, properties and uses in biomaterials, Acta Biomater. 6(9) (2010) 3362–3378. https://doi.org/10.1016/j.actbio.2010.02.017.

23. E. Eanes, Amorphous Calcium Phosphate, in: Octacalcium Phosphate, (2001) 130–147. https://doi.org/10.1159/000061652.

24. M. Vallet-Regí, D. Lozano, B. González, I. Izquierdo-Barba, Biomaterials against Bone Infection, Adv. Healthc. Mater. 9(13) (2020). https://doi.org/10.1002/adhm.202000310.

25. H. Tabaja, O. M. Abu Saleh, D. R. Osmon, Periprosthetic Joint Infection: What's New? Infect. Dis. Clin. North. Am. 38(4) (2024) 731–756. https://doi.org/10.1016/J.IDC.2024.07.007.

26. L. Pulido, E. Ghanem, A. Joshi, J. J. Purtill, J. Parvizi, Periprosthetic Joint Infection: The Incidence, Timing, and Predisposing Factors, Clin. Orthop. Relat. Res. 466(7) (2008) 1710–1715. https://doi.org/10.1007/S11999-008-0209-4.

27. V. Boddapati, M. C. Fu, D. J. Mayman, E. P. Su, P. K. Sculco, A. S. McLawhorn, Revision Total Knee Arthroplasty for Periprosthetic Joint Infection Is Associated with Increased Postoperative Morbidity and Mortality Relative to Noninfectious Revisions, J. Arthroplasty. 33(2) (2018) 521–526. https://doi.org/10.1016/J.ARTH.2017.09.021.

28. F. Der Wang, Y. P. Wang, C. F. Chen, H. P. Chen, The incidence rate, trend and microbiological aetiology of prosthetic joint infection after total knee arthroplasty: A 13 years' experience from a tertiary medical center in Taiwan, Journal of Microbiology, Immunology and Infection. 51(6) (2018) 717–722. https://doi.org/10.1016/J.JMII.2018.08.011.

29. O. F. Egerci, A. Yapar, F. Dogruoz, H. Selcuk, O. Kose, Preventive strategies to reduce the rate of periprosthetic infections in total joint arthroplasty; a comprehensive review, Archives of Orthopaedic and Trauma Surgery. 144 (2024) 5131–5146. https://doi.org/10.1007/S00402-024-05301-W.

30. M. Riool, S. A. J. Zaat, Biomaterial-Associated Infection: Pathogenesis and Prevention, In: Soria, F., Rako, D., de Graaf, P. (eds) Urinary Stents. Springer (2022) 245–257. https://doi.org/10.1007/978-3-031-04484-7_20.

31. D. Y. Wang, L. Su, K. Poelstra, D. W. Grainger, H. C. van der Mei, L. Shi, H. J. Busscher, Beyond surface modification strategies to control infections associated with implanted biomaterials and devices – Addressing the opportunities offered by nanotechnology, Biomaterials. 308 (2024) 122576. https://doi.org/10.1016/J.BIOMATERIALS.2024.122576.

32. J. Barros, F. J. Monteiro, M. P. Ferraz, Bioengineering Approaches to Fight against Orthopedic Biomaterials Related-Infections, Int. J. Mol. Sci. 23(19) (2022) 11658. https://doi.org/10.3390/ijms231911658.

33. W. Shuaishuai, Z. Tongtong, W. Dapeng, Z. Mingran, W. Xukai, Y. Yue, D. Hengliang, W. Guangzhi, Z. Minglei, Implantable biomedical materials for treatment of bone infection, Front. Bioeng. Biotechnol. 11 (2023). https://doi.org/10.3389/fbioe.2023.1081446.

34. M. Cerioli, C. Batailler, A. Conrad, S. Roux, T. Perpoint, A. Becker, C. Triffault-Fillit, S. Lustig, M.-H. Fessy, F. Laurent, F. Valour, C. Chidiac, T. Ferry, Pseudomonas aeruginosa Implant-Associated Bone and Joint Infections: Experience in a Regional Reference Center in France, Front Med. 7 (2020). https://doi.org/10.3389/fmed.2020.513242.

35. A. Frei, A. D. Verderosa, A. G. Elliott, J. Zuegg, M. A. T. Blaskovich, Metals to combat antimicrobial resistance, Nature Reviews Chemistry. 7 (2023) 202–224. https://doi.org/10.1038/s41570-023-00463-4.

36. M. Godoy-Gallardo, U. Eckhard, L. M. Delgado, Y. J. D. de Roo Puente, M. Hoyos-Nogués, F. J. Gil, R. A. Perez, Antibacterial approaches in tissue engineering using metal ions and nanoparticles: From mechanisms to applications, Bioact. Mater. 6(12) (2021) 4470. https://doi.org/10.1016/J.BIOACTMAT.2021.04.033.

37. J. A. Lemire, J. J. Harrison, R. J. Turner, Antimicrobial activity of metals: Mechanisms, molecular targets and applications, Nat. Rev. Microbiol. 11 (2013) 371–384. https://doi.org/10.1038/nrmicro3028.

38. S. Mittapally, R. Taranum, S. Parveen, Metal ions as antibacterial agents, Journal of Drug Delivery and Therapeutics. 8(6) (2018) 411–419. https://doi.org/10.22270/JDDT.V8I6-S.2063.

39. M. A. Zoroddu, J. Aaseth, G. Crisponi, S. Medici, M. Peana, V. M. Nurchi, The essential metals for humans: a brief overview, J. Inorg. 195 (2019) 120–129. https://doi.org/10.1016/j.jinorgbio.2019.03.013.

40. A. B. Kelson, M. Carnevali, V. Truong-Le, Gallium-based anti-infectives: Targeting microbial iron-uptake mechanisms, Curr. Opin. Pharmacol. 5(13) (2013) 707–716. https://doi.org/10.1016/j.coph.2013.07.001.

41. F. Kurtuldu, N. Mutlu, A. R. Boccaccini, D. Galusek, Gallium containing bioactive materials: A review of anticancer, antibacterial, and osteogenic properties, Bioact. Mater. 17 (2022) 125–146. https://doi.org/10.1016/j.bioactmat.2021.12.034.

42. V. Vitali, S. Zineddu, L. Messori, Metal compounds as antimicrobial agents: ‘smart’ approaches for discovering new effective treatments, RSC Adv. 15 (2025) 748–753. https://doi.org/10.1039/D4RA07449A.

43. P. Collery, B. Keppler, C. Madoulet, B. Desoize, Gallium in cancer treatment, Crit. Rev. Oncol. Hematol. 42(3) (2002) 283–296. https://doi.org/10.1016/S1040-8428(01)00225-6.

44. V. de A. W. Sales, T. R. R. Timóteo, N. M. da Silva, C. G. de Melo, A. S. Ferreira, M. V. G. de Oliveira, E. de O. Silva, L. M. dos S. Mendes, L. A. Rolim, P. J. R. Neto, A Systematic Review of the Anti-inflammatory Effects of Gallium Compounds, Curr. Med. Chem. 28(10) (2020) 2062–2076. https://doi.org/10.2174/0929867327666200525160556.

45. W. Sun, M. Qi, S. Cheng, C. Li, B. Dong, L. Wang, Gallium and gallium compounds: New insights into the “Trojan horse” strategy in medical applications, Mater. Des. 227 (2023) 111704. https://doi.org/10.1016/J.MATDES.2023.111704.

46. F. Li, F. Liu, K. Huang, S. Yang, Advancement of Gallium and Gallium-Based Compounds as Antimicrobial Agents, Front. Bioeng. Biotechnol. 10 (2022) 827960. https://doi.org/10.3389/FBIOE.2022.827960.

47. F. Shi, S. S. Ma, S. Liu, R. Xin, B. Chen, W. Ye, J. Sun, A novel antimicrobial strategy for bacterial infections: Gallium-based materials, Colloid Interface Sci. Commun. 56 (2023) 100735. https://doi.org/10.1016/J.COLCOM.2023.100735.

48. B. R. Wilson, A. R. Bogdan, M. Miyazawa, K. Hashimoto, Y. Tsuji, Siderophores in Iron Metabolism: From Mechanism to Therapy Potential, Trends Mol Med. 22(12) (2016) 1077–1090. https://doi.org/10.1016/j.molmed.2016.10.005.

49. N. Kircheva, T. Dudev, Gallium as an Antibacterial Agent: A DFT/SMD Study of the Ga3+/Fe3+ Competition for Binding Bacterial Siderophores, Inorg. Chem. 59(9) (2020) 6242–6254. https://doi.org/10.1021/acs.inorgchem.0c00367.

50. A. Müller, C. Fessele, F. Zuber, M. Rottmar, K. Maniura-Weber, Q. Ren, A. G. Guex, Gallium Complex-Functionalized P4HB Fibers: A Trojan Horse to Fight Bacterial Infection, ACS Appl. Bio. Mater. 4(1) (2021) 682–691. https://doi.org/10.1021/acsabm.0c01221.

51. F. Minandri, C. Bonchi, E. Frangipani, F. Imperi, P. Visca, Promises and failures of gallium as an antibacterial agent, Future Microbiol. 9(3) (2014) 379–397. https://doi.org/10.2217/fmb.14.3.

52. M. Mosina, I. Kovrlija, L. Stipniece, J. Locs, Gallium containing calcium phosphates: Potential antibacterial agents or fictitious truth, Acta Biomater. 150 (2022) 48–57. https://doi.org/10.1016/j.actbio.2022.07.063.

53. M. Yang, J. Ren, R. Zhang, Novel gallium-doped amorphous calcium phosphate nanoparticles: Preparation, application and structure study, J. Non-Cryst. Solids. 466–467 (2017) 15–20. https://doi.org/10.1016/j.jnoncrysol.2017.03.034.

54. M. Kurtjak, M. Vukomanović, A. Krajnc, L. Kramer, B. Turk, D. Suvorov, Designing Ga(III)-containing hydroxyapatite with antibacterial activity, RSC Adv. 6 (2016) 112839–112852. https://doi.org/10.1039/c6ra23424k.

55. K. Pajor, Ł. Pajchel, A. Zgadzaj, U. Piotrowska, J. Kolmas, Modifications of hydroxyapatite by gallium and silver ions—physicochemical characterization, cytotoxicity and antibacterial evaluation, Int. J. Mol. Sci. 21(14) (2020) 5006. https://doi.org/10.3390/ijms21145006.

56. M. Kurtjak, M. Vukomanović, D. Suvorov, Antibacterial nanocomposite of functionalized nanogold and gallium-doped hydroxyapatite, Mater. Lett. 193 (2017) 126–129. https://doi.org/10.1016/j.matlet.2017.01.092.

57. C. Combes, C. Rey, Amorphous calcium phosphates: Synthesis, properties and uses in biomaterials, Acta Biomater. 6(9) (2010) 3362–3378. https://doi.org/https://doi.org/10.1016/j.actbio.2010.02.017.

58. S. V. Dorozhkin, Synthetic amorphous calcium phosphates (ACPs): Preparation, structure, properties, and biomedical applications, Biomater. Sci. 9 (2021) 7748–7798. https://doi.org/https://doi.org/10.1039/d1bm01239h.

59. M. Mosina, J. Locs, Synthesis of Amorphous Calcium Phosphate: A Review, Key Eng. Mater. 850 (2020) 199–206. https://doi.org/10.4028/www.scientific.net/KEM.850.199.

60. J. Vecstaudza, J. Locs, Novel preparation route of stable amorphous calcium phosphate nanoparticles with high specific surface area, J. Alloys Compd. 700 (2017) 215–222. https://doi.org/http://dx.doi.org/10.1016/j.jallcom.2017.01.038.

61. G. Mancardi, C. E. Hernandez Tamargo, D. Di Tommaso, N. H. De Leeuw, Detection of Posner's clusters during calcium phosphate nucleation: a molecular dynamics study, J. Mater. Chem. B. 5 (2017) 7274–7284. https://doi.org/10.1039/C7TB01199G.

62. S. Somrani, C. Rey, M. Jemal, Thermal evolution of amorphous tricalcium phosphate, J. Mater. Chem. 13 (2003) 888–892. https://doi.org/10.1039/B210900J.

63. L. Degli Esposti, M. Fosca, A. Canizares, L. Del Campo, M. Ortenzi, A. Adamiano, J. V. Rau, M. Iafisco, An in situ study of thermal crystallization of amorphous calcium phosphates, Physical Chemistry Chemical Physics. 24 (2022) 24514–24523. https://doi.org/10.1039/D2CP02352K.

64. L. Degli Esposti, S. Markovic, N. Ignjatovic, S. Panseri, M. Montesi, A. Adamiano, M. Fosca, J. V. Rau, V. Uskoković, M. Iafisco, Thermal crystallization of amorphous calcium phosphate combined with citrate and fluoride doping: a novel route to produce hydroxyapatite bioceramics, J. Mater. Chem. B. 9 (2021) 4832–4845. https://doi.org/10.1039/D1TB00601K.

65. Z. Z. Zyman, A. V. Goncharenko, D. V. Rokhmistrov, Phase evolution during heat treatment of amorphous calcium phosphate derived from fast nitrate synthesis, Processing and Application of Ceramics. 11(2) (2017) 147–153. https://doi.org/10.2298/PAC1702147Z.

66. J. Vecstaudza, M. Gasik, J. Locs, Amorphous calcium phosphate materials: Formation, structure and thermal behaviour, J. Eur. Ceram. Soc. 39(4) (2019) 1642–1649. https://doi.org/10.1016/J.JEURCERAMSOC.2018.11.003.

67. W. Jin, S. Jiang, H. Pan, R. Tang, Amorphous Phase Mediated Crystallization: Fundamentals of Biomineralization, Crystals. 8(1) (2018) 48. https://doi.org/10.3390/CRYST8010048.

68. E. D. Eanes, J. D. Termine, M. U. Nylen, An electron microscopic study of the formation of amorphous calcium phosphate and its transformation to crystalline apatite, Calcif Tissue Res. 12 (1973) 143–158. https://doi.org/10.1007/BF02013730.

69. B. Jin, Z. Liu, C. Shao, J. Chen, L. Liu, R. Tang, J. J. De Yoreo, Phase Transformation Mechanism of Amorphous Calcium Phosphate to Hydroxyapatite Investigated by Liquid-Cell Transmission Electron Microscopy, Cryst. Growth Des. 21(9) (2021) 5126–5134. https://doi.org/10.1021/acs.cgd.1c00503.

70. K. Chatzipanagis, M. Iafisco, T. Roncal-Herrero, M. Bilton, A. Tampieri, R. Kröger, J. M. Delgado-López, Crystallization of citrate-stabilized amorphous calcium phosphate to nanocrystalline apatite: a surface-mediated transformation, Cryst. Eng. Comm. 18 (2016) 3170–3173. https://doi.org/10.1039/C6CE00521G.

71. H. Saito, Y. Araki, H. Katsuno, T. Nakada, Phase transition of amorphous calcium phosphate to calcium hydrogen phosphate dihydrate in simulated body fluid, J. Cryst. Growth. 553 (2021) 125937. https://doi.org/10.1016/J.JCRYSGRO.2020.125937.

72. M. Edén, Structure and formation of amorphous calcium phosphate and its role as surface layer of nanocrystalline apatite: Implications for bone mineralization, Materialia (Oxf) 17 (2021) 101107. https://doi.org/10.1016/j.mtla.2021.101107.

73. A. Indurkar, P. Kudale, V. Rjabovs, I. Heinmaa, Ö. Demir, M. Kirejevs, K. Rubenis, G. Chaturbhuj, M. Turks, J. Locs, Small organic molecules containing amorphous calcium phosphate: synthesis, characterization and transformation, Front. Bioeng. Biotechnol. 11 (2023) 1329752. https://doi.org/10.3389/FBIOE.2023.1329752.

74. R. Gelli, F. Ridi, P. Baglioni, The importance of being amorphous: calcium and magnesium phosphates in the human body, Adv. Colloid. Interface Sci. 269 (2019) 219–235. https://doi.org/10.1016/j.cis.2019.04.011.

75. S. Jiang, Y. Cao, S. Li, Y. Pang, Z. Sun, Dual function of poly(acrylic acid) on controlling amorphous mediated hydroxyapatite crystallization, J. Cryst. Growth. 557 (2021) 125991. https://doi.org/10.1016/J.JCRYSGRO.2020.125991.

76. V. M. Wu, E. Huynh, S. Tang, V. Uskoković, Calcium phosphate nanoparticles as intrinsic inorganic antimicrobials: Mechanism of action, Biomedical Materials (Bristol) 16 (2021) 015018. https://doi.org/10.1088/1748-605X/ABA281.

77. I. I. Grynyuk, O. M. Vasyliuk, S. V. Prylutska, N. Y. Strutynska, O. V. Livitska, M. S. Slobodyanik, Influence of nanoscale-modified apatite-type calcium phosphates on the biofilm formation by pathogenic microorganisms, Open Chem. 19 (2021) 39–48. https://doi.org/10.1515/CHEM-2021-0199.

78. V. Uskoković, S. Tang, M. G. Nikolić, S. Marković, V. M. Wu, Calcium phosphate nanoparticles as intrinsic inorganic antimicrobials: In search of the key particle property, Biointerphases. 14 (2019) 031001. https://doi.org/10.1116/1.5090396.

79. A. Bondi, Van der Waals volumes and radii, Journal of Physical Chemistry. 68 (1964) 441–451. https://doi.org/10.1021/J100785A001.

80. N. C. Blumenthal, V. Cosma, S. Levine, Effect of gallium on the in vitro formation, growth, and solubility of hydroxyapatite, Calcif Tissue Int. 45 (1989) 81–87. https://doi.org/10.1007/BF02561406.

81. Y. In, U. Amornkitbamrung, M. H. Hong, H. Shin, On the crystallization of hydroxyapatite under hydrothermal conditions: Role of sebacic acid as an additive, ACS Omega. 5(42) (2020) 27204–27210. https://doi.org/10.1021/acsomega.0c03297.

82. M. Mosina, C. Siverino, L. Stipniece, A. Sceglovs, R. Vasiljevs, T. F. Moriarty, J. Locs, Gallium-Doped Hydroxyapatite Shows Antibacterial Activity against Pseudomonas aeruginosa without Affecting Cell Metabolic Activity, J. Funct. Biomater. 14(2) (2023) 51. https://doi.org/10.3390/jfb14020051.

83. A. Ballardini, M. Montesi, S. Panseri, A. Vandini, P.G. Balboni, A. Tampieri, S. Sprio, New hydroxyapatite nanophases with enhanced osteogenic and anti-bacterial activity, J. Biomed. Mater. Res. A. 106(2) (2017) 521–530. https://doi.org/10.1002/jbm.a.36249.

84. F. He, Y. Tian, Improvements in phase stability and densification of β-tricalcium phosphate bioceramics by strontium-containing phosphate-based glass additive, Ceram. Int. 44(10) (2018) 11622–11627. https://doi.org/10.1016/j.ceramint.2018.03.236.

85. J. Liu, L. Zhao, L. Ni, C. Qiao, D. Li, H. Sun, Z. Zhang, The effect of synthetic α-tricalcium phosphate on osteogenic differentiation of rat bone mesenchymal stem cells, Am. J. Transl. Res. 7(9) (2015) 1588–1601. https://www.ncbi.nlm.nih.gov/pmc/articles/PMC4626420/.

86. M. Trzaskowska, V. Vivcharenko, A. Przekora, The Impact of Hydroxyapatite Sintering Temperature on Its Microstructural, Mechanical, and Biological Properties, Int. J. Mol. Sci. 24(6) (2023) 5083. https://doi.org/10.3390/ijms24065083.

87. K. Salma, N. Borodajenko, A. Plata, L. Berzina-Cimdina, A. Stunda, Fourier Transform Infrared Spectra of Technologically Modified Calcium Phosphates, in 14th Nordic-Baltic Conference on Biomedical Engineering and Medical Physics, IFMBE Proceedings, 20 (2008) 68–71. https://doi.org/10.1007/978-3-540-69367-3_19.

88. D. Fan, L. Q. Chen, S. P. P. Chen, Numerical simulation of Zener pinning with growing second-phase particles, Journal of the American Ceramic Society. 81(3) (2005) 526–532. https://doi.org/10.1111/j.1151-2916.1998.tb02370.x.

89. M. Sceglova, N. Döbelin, R. Vasiljevs, L. Stipniece, J. Locs. Influence of gallium doping on the thermal stability and microstructure of sintered hydroxyapatite bioceramics, Ceram. Int. 51(14) (2025) 41150-42261. https://doi.org/10.1016/j.ceramint.2025.06.440

Marika Ščeglova was born in 1994 in Riga, Latvia. She obtained a Bachelor's degree in Engineering (2018) and a Master's degree in Engineering in Chemical Technology (2020) from Riga Technical University (RTU). From 2013 to 2018, she worked at JSC Grindeks. From 2018 to 2025, she was a researcher at the Institute of Biomaterials and Bioengineering, Faculty of Natural Sciences and Technology, RTU. Her research interests focus on calcium phosphate biomaterials and their modification with various ions to improve physicochemical and biological properties. The results of her research have been presented at international scientific conferences and published in scientific journals. Currently, she works as a chemistry teacher.